nature microbiology

LETTERS

https://doi.org/10.1038/s41564-020-00824-5

Check for updates

Spike-specific circulating T follicular helper cell and cross-neutralizing antibody responses in COVID-19-convalescent individuals

Jian Zhang[1,15], Qian Wu[1,15], Ziyan Liu[1,15], Qijie Wang[2,15], Jiajing Wu[3,4,15], Yabin Hu[1,15], Tingting Bai[5], Ting Xie[2], Mincheng Huang[2], Tiantian Wu[6], Danhong Peng[2], Weijin Huang[3], Kun Jin[1], Ling Niu[1], Wangyuan Guo[1], Dixian Luo[1], Dongzhu Lei[1], Zhijian Wu[1], Guicheng Li[1], Renbin Huang[1], Yingbiao Lin[1], Xiangping Xie[2], Shuangyan He[2], Yunfan Deng[7], Jianghua Liu[8], Weilang Li[9], Zhongyi Lu[10], Haifu Chen[11], Ting Zeng[2], Qingting Luo[12], Yi-Ping Li[6] ✉, Youchun Wang[3] ✉, Wenpei Liu[1,5,13] ✉ and Xiaowang Qu[1,14] ✉

Coronavirus disease 2019 (COVID-19) is caused by infection with severe acute respiratory syndrome coronavirus 2 (SARS-CoV-2)[1–3] and individuals with COVID-19 have symptoms that can be asymptomatic, mild, moderate or severe[4,5]. In the early phase of infection, T- and B-cell counts are substantially decreased[6,7]; however, IgM[8–11] and IgG[12–14] are detectable within 14 d after symptom onset. In COVID-19-convalescent individuals, spike-specific neutralizing antibodies are variable[3,15,16]. No specific drug or vaccine is available for COVID-19 at the time of writing; however, patients benefit from treatment with serum from COVID-19-convalescent individuals[17,18]. Nevertheless, antibody responses and cross-reactivity with other coronaviruses in COVID-19-convalescent individuals are largely unknown. Here, we show that the majority of COVID-19-convalescent individuals maintained SARS-CoV-2 spike S1- and S2-specific antibodies with neutralizing activity against the SARS-CoV-2 pseudotyped virus, and that some of the antibodies cross-neutralized SARS-CoV, Middle East respiratory syndrome coronavirus or both pseudotyped viruses. Convalescent individuals who experienced severe COVID-19 showed higher neutralizing antibody titres, a faster increase in lymphocyte counts and a higher frequency of CXCR3$^+$ T follicular help (T_{FH}) cells compared with COVID-19-convalescent individuals who experienced non-severe disease. Circulating T_{FH} cells were spike specific and functional, and the frequencies of CXCR3$^+$ T_{FH} cells were positively associated with neutralizing antibody titres in COVID-19-convalescent individuals. No individuals had detectable autoantibodies. These findings provide insights into neutralizing antibody responses in COVID-19-convalescent individuals and facilitate the treatment and vaccine development for SARS-CoV-2 infection.

To investigate the antibody response after recovery from coronavirus disease 2019 (COVID-19), 67 convalescent individuals were recruited for this study, and blood was drawn on day 28 after discharge. The baseline clinical characteristics and laboratory findings on admission were retrospectively analysed (Extended Data Figs. 1 and 2). The binding and avidity of an antibody to a specific antigen reflect the overall strength and quality of the antibody. To assess the reactivity of COVID-19 serum antibodies, the binding activity and avidity of the serum to severe acute respiratory syndrome coronavirus 2 (SARS-CoV-2) spike subunits S1 and S2 were examined using a human-IgG-specific enzyme-linked immunosorbent assay (ELISA). The results showed that all 67 sera contained anti-S1 (median titre = 4.61; interquartile range (IQR) = 4.01–4.61) and anti-S2 (median titre = 4.91; IQR = 4.61–5.52) IgG antibodies (Fig. 1a and Extended Data Fig. 3). Furthermore, the end-point titres of anti-S1 and anti-S2 antibodies were positively correlated (Extended Data Fig. 4a). To evaluate binding specificity, 61 sera collected from healthy control individuals were examined in parallel, and only one serum sample (1/61, 1.6%) was found to have binding activity against SARS-CoV-2 spike S1 but not S2 (Extended Data Fig. 5). Similar patterns were observed for antibody avidity, in which 64 out of 67 sera (3 sera were excluded as they did not meet the requirements for the avidity assay) exhibited medium avidity to S1 (median = 44.50; IQR = 34.50–51.75) and S2 (median = 58.00; IQR = 49.00–67.00; Fig. 1b and Extended Data Fig. 3). These data indicate that the majority of the COVID-19-convalescent individuals elicited and maintained robust SARS-CoV-2 spike-specific IgG antibodies with a medium avidity.

[1]Translational Medicine Institute, The First People's Hospital of Chenzhou, University of South China, Chenzhou, China. [2]The Central Hospital of Shaoyang, Shaoyang, China. [3]National Institutes for Food and Drug Control, Key Laboratory of the Ministry of Health for Research on Quality and Standardization of Biotech Products, Key Laboratory of Biological Product Quality Research and Evaluation of National Medical Products Administration, Beijing, China. [4]Wuhan Institute of Biological Products, Wuhan, China. [5]The First School of Clinical Medicine, Southern Medical University, Guangzhou, China. [6]Institute of Human Virology, Zhongshan School of Medicine, and Key Laboratory of Tropical Disease Control of Ministry of Education, Sun Yat-sen University, Guangzhou, China. [7]The Longhui People's Hospital, Longhui, China. [8]The Xinshao People's Hospital, Xinshao, China. [9]The Dongkou People's Hospital, Dongkou, China. [10]The Shaoyang People's Hospital, Shaoyang, China. [11]The Suining People's Hospital, Suining, China. [12]The Baoqing Psychiatric Hospital, Shaoyang, China. [13]School of Laboratory Medicine and Biotechnology, Southern Medical University, Guangzhou, China. [14]School of Public Health, Southern Medical University, Guangzhou, China. [15]These authors contributed equally: Jian Zhang, Qian Wu, Ziyan Liu, Qijie Wang, Jiajing Wu, Yabin Hu. ✉e-mail: lyiping@mail.sysu.edu.cn; wangyc@nifdc.org.cn; wenpeiliu_2008@foxmail.com; quxiaowang@163.com

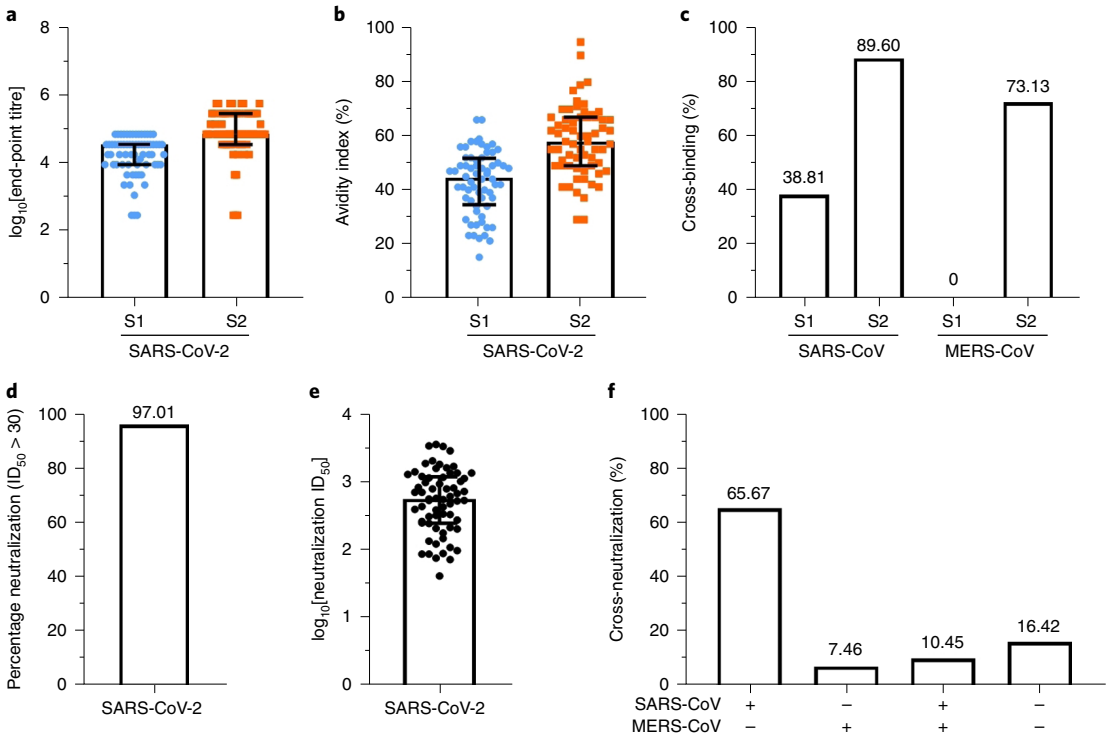

Fig. 1 | The majority of individuals who have recovered from COVID-19 maintain neutralizing antibodies, some of which cross-bind to and neutralize SARS-CoV and/or MERS-CoV. a, End-point dilution titre of serum IgG antibodies from individuals who recovered from COVID-19 ($n = 67$), determined by antibody binding to SARS-CoV-2 spike subunits S1 and S2 and shown as final dilution titres. **b**, The avidity of serum IgG antibodies to SARS-CoV-2 spike subunits S1 and S2 ($n = 64$), shown as avidity index. **c**, The percentage of sera derived from COVID-19-convalescent individuals with cross-binding activity to spike subunits S1 and S2 from both SARS-CoV and MERS-CoV. **d**, The percentage of sera derived from COVID-19-convalescent individuals that neutralizes SARS-CoV-2 pseudotyped virus ($ID_{50} > 30$) ($n = 65/67$, 97.01%). **e**, Neutralization titre of sera derived from COVID-19-convalescent individuals against SARS-CoV-2 pseudotyped virus (ID_{50}, $n = 65$). **f**, The percentage of the SARS-CoV-2-neutralizing sera ($n = 65$) that shows cross-neutralization against pseudotyped viruses of SARS-CoV and MERS-CoV. The plus and minus symbols indicate with and without cross-neutralization, respectively. For **a** and **e**, end-point titres and neutralization titres were log_{10}-transformed. For **a**, **b**, and **e**, data are median ± IQR (25–75%).

The cross-reactivity of antibodies has been reported for coronaviruses, as sera from recovered SARS individuals showed cross-reaction with Middle East respiratory syndrome coronavirus (MERS-CoV)[19]. SARS-CoV-2 shows high sequence homology with SARS-CoV and less similarity to MERS-CoV[2,3]. To examine whether the serum antibodies derived from COVID-19-convalescent individuals cross-react with other coronaviruses, a binding assay was performed using spike subunits S1 and S2 from both SARS-CoV and MERS-CoV. The results showed that 38.81% (26/67) and 89.55% (60/67) of the sera bound to SARS-CoV S1 and S2, respectively (Fig. 1c and Extended Data Fig. 3). For MERS-CoV, no binding was detected for S1, whereas 73.13% (49/67) of the sera bound to S2 (Fig. 1c and Extended Data Fig. 3). As negative controls, 61 healthy sera were included in each experiment, and no cross-binding was found for SARS-CoV S1. Only 1.67% (1/61), 6.66% (4/61) and 1.67% (1/61) of the sera showed binding activity to SARS-CoV S2, MERS-CoV S1 and MERS-CoV S2, respectively (Extended Data Fig. 5). These results suggest that COVID-19-convalescent individuals elicited antibodies with cross-binding activity to SARS-CoV and MERS-CoV.

Next, sera neutralization of SARS-CoV-2 and its cross-neutralization of SARS-CoV and MERS-CoV were determined. SARS-CoV-2 pseudotyped virus was constructed and used for neutralization[20], and previously developed SARS-CoV and MERS-CoV pseudotyped viruses were used for cross-neutralization[21]. The results showed that 97.01% (65/67) of the sera from individuals who had recovered from COVID-19 contained neutralizing antibodies that efficiently neutralized SARS-CoV-2 pseudotyped virus (50% inhibitory dilution (ID_{50}) = 2.75; IQR = 2.34–3.08; Fig. 1d,e and Extended Data Fig. 3), and the neutralization titres were positively correlated with the end-point binding titres of anti-S1 and anti-S2 antibodies (Extended Data Fig. 4b,c). Cross-neutralization was observed and variable for different viruses; 65.67% (44/67), 7.46% (5/67) and 10.45% (7/67) of the sera cross-neutralized SARS-CoV, MERS-CoV and both viruses, respectively. Furthermore, 16.42% (11/67) of the sera showed no cross-neutralization activity (Fig. 1f and Extended Data Fig. 3). However, having cross-neutralization activity did not seem to affect the ability of a serum to neutralize SARS-CoV-2, as the serum groups with and without cross-neutralization activity showed no significant difference in the neutralization titres for SARS-CoV-2 (Extended Data Fig. 6a). Similarly, neutralization titres for SARS-CoV-2 were also comparable between those sera that cross-neutralized SARS-CoV, MERS-CoV or both viruses (Extended Data Fig. 6b). Nevertheless, cross-neutralization titres for SARS-CoV and MERS-CoV were significantly lower than their neutralization titres for SARS-CoV-2 in general (Extended Data Fig. 6c–e). Furthermore, autoantibodies were not detectable in the tested sera derived from COVID-19-convalescent individuals (Extended Data Fig. 7). These findings demonstrate that the majority of patients with COVID-19 elicited and maintained robust neutralizing antibody responses to SARS-CoV-2 after recovery; the serum of some convalescent individuals also contained antibodies with cross-binding and neutralizing activities to SARS-CoV, MERS-CoV or both coronaviruses.

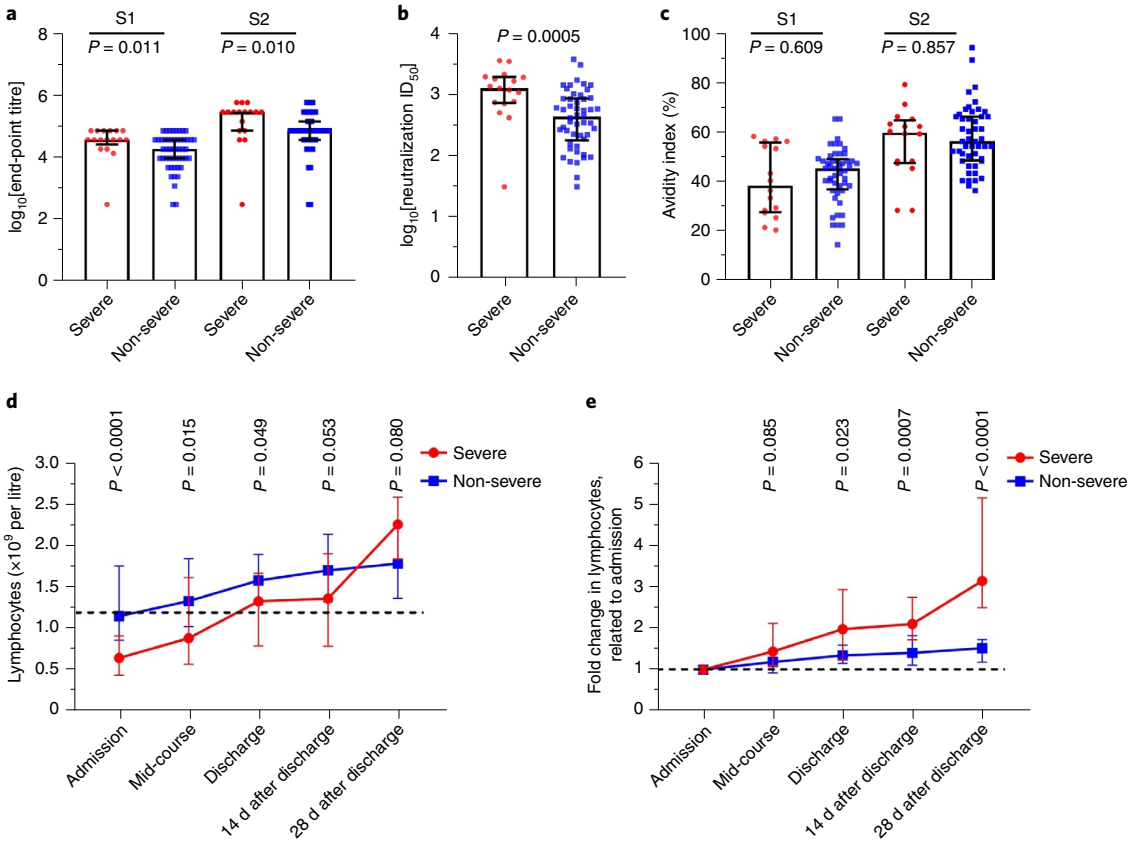

Fig. 2 | Convalescent individuals who experienced severe COVID-19 symptoms show a higher neutralizing antibody response and an accelerated recovery rate of lymphocytes compared with those who had non-severe symptoms. a, Comparison of end-point titres of SARS-CoV-2 spike S1- and S2-specific IgG antibodies from COVID-19-convalescent individuals who had experienced severe ($n=17$) and non-severe ($n=50$) symptoms. **b**, Comparison of neutralization titres to SARS-CoV-2 pseudotyped virus for the sera from convalescent individuals who had severe ($n=17$) and non-severe ($n=50$) COVID-19. **c**, Comparison of avidity indexes of SARS-CoV-2 spike S1- and S2-specific IgG antibodies derived from convalescent individuals who had severe ($n=16$) and non-severe ($n=48$) COVID-19. **d**,**e**, The kinetics of lymphocyte counts (**d**) and the fold change in lymphocytes relative to admission for the time points as indicated (**e**) for the severe (red, circle) and non-severe (blue, square) groups of convalescent individuals, in which the number of patients included in the analysis was as follows (severe versus non-severe): on admission ($n=17$ versus $n=50$), mid-course of disease ($n=17$ versus $n=41$), discharge ($n=16$ versus $n=30$), 14 d after discharge ($n=13$ versus $n=40$) and 28 d after discharge ($n=13$ versus $n=40$). For **a** and **b**, end-point titres and neutralization titres were logarithmically transformed. In **d** and **e**, the dotted lines indicate the bottom line of the normal range of lymphocyte count and the baseline of the fold change in lymphocytes related to admission, respectively. For **a**–**e**, data are median ± IQR (25–75%). Mann–Whitney *U*-tests were used to analyse the difference between two groups; $P<0.05$ was considered to be a two-tailed significant difference.

It has been reported that patients with COVID-19 with severe and mild symptoms showed distinct clinical and immunological presentations[5,17,18]. To study whether the severity of COVID-19 symptoms that patients experienced affects the neutralizing antibody responses after disease recovery, 67 convalescent individuals were categorized into severe (17/67) and non-severe (50/67) groups, according to the severity of disease that the patients had (Extended Data Fig. 1). Compared with the non-severe group, the severe group exhibited higher end-point titres of antibodies, anti-S1 ($P=0.011$) and anti-S2 ($P=0.010$; Fig. 2a) antibodies, and neutralization titres ($P<0.001$) to SARS-CoV-2 (Fig. 2b). However, in the severe and non-severe groups, there was no difference in the avidity indexes of either anti-S1 ($P=0.609$) or anti-S2 ($P=0.857$; Fig. 2c) antibodies. Although the severe group had an older age ($P<0.001$), a longer course of disease ($P=0.007$), more comorbidities ($P=0.044$) and a higher total of underlying diseases ($P<0.001$) compared with the non-severe group (Extended Data Fig. 1), multivariable analysis of the factors that may be associated with neutralizing antibody responses revealed that neutralizing antibody titres were correlated with the severity of disease (odds ratio (OR) = 5.04, 95% confidence interval (CI) = 1.003–25.30; Table 1).

As the neutralizing antibody responses are essentially related to the functional lymphocytes, the lymphocyte kinetics in severe and non-severe groups were therefore investigated from admission to recovery phase at the following five time points: admission, mid-course, discharge, day 14 and day 28 after discharge (Fig. 2d). The results revealed that the majority of the severe group (16/17, 94.12%) had lower lymphocyte counts at the first four time-points ($P\leq0.05$). This observation is consistent with those of a recent report, in which patients with severe COVID-19 showed decreased T- and B-cell counts[4], and lymphopaenia was often observed on admission, especially for those with severe symptoms[4,7]. Here, lymphocyte counts of the non-severe group on admission were close to the bottom line of the normal range (Fig. 2d). Lymphocyte counts of both groups increased gradually, and the severe group was restored to a normal level on discharge (median, from 0.65 to 2.28×10^9 per litre) and maintained this level for two weeks. From day 14 to day 28 after discharge, lymphocyte counts of the severe group increased

Table 1 | Analysis of impact factors on neutralization antibody

Analysis	Univariate (OR (95% CI))	Multivariable (OR (95% CI))
Course of disease	3.67 (1.34–10.06)	2.14 (0.67–6.78)
Severity of disease	7.00 (1.78–27.53)	5.04 (1.003–25.300)
Comorbidities	3.33 (1.20–9.29)	0.43 (0.13–1.42)
Underlying disease	2.78 (0.98–7.88)	0.77(0.19–3.17)

rapidly and reached a mean value that was higher than that of the non-severe group ($P=0.08$; Fig. 2d). Although lymphocyte counts of both groups increased, the severe group showed higher fold changes at all time points, related to admission, compared with the non-severe group ($P<0.01$; Fig. 2e), suggesting that convalescent individuals who had severe COVID-19 have higher restoration rates of lymphocytes, which may contribute to antibody maintenance and neutralizing antibody responses.

T_{FH} cells, a T-cell subset, have been identified as professional B helper T cells in past decades and are required for T-dependent antibody production[22,23]. Circulating T_{FH} cells are representative of germinal centre T_{FH} cells and have an important role in T-dependent B-cell maturation and antibody production[24]. As the severe group had higher antibody titres in binding and neutralization (Fig. 2a,b), as well as a faster increase in lymphocyte counts (Fig. 2d), it is interesting to investigate whether the T_{FH} cells of lymphocytes are correlated with the neutralization effect. Circulating T_{FH} cells were analysed by gating on PD-1$^+$CXCR5$^+$CD4$^+$ T cells (Extended Data Fig. 8a). Analysis of the frequency of total circulating T_{FH} cells showed that COVID-19-convalescent individuals and healthy controls had no difference in the frequency of total T_{FH} cells (Extended Data Fig. 8b); however, the frequency of CXCR3$^+$ T_{FH}-cell subsets in total T_{FH} cells of COVID-19-convalescent individuals (both severe and non-severe groups) was lower compared with that of healthy controls (Extended Data Fig. 8c–e). When analysed by severe, non-severe and healthy control groups, total T_{FH} cells were comparable among three groups (Fig. 3a); however, similar to the healthy control group, the severe group showed a higher frequency of CXCR3$^+$ T_{FH} cells compared with the non-severe group ($P=0.006$). Accordingly, the frequency of CXCR3$^-$ T_{FH} cells ($P=0.001$) and the ratio of CXCR3$^+$/CXCR3$^-$ T_{FH} cells ($P=0.013$) were lower and higher compared with the non-severe group, respectively (Fig. 3b–d). Correlation coefficient analysis revealed that the frequency of total T_{FH} cells had no correlation with neutralization titres (ID_{50}; $r=-0.004$, $P=0.985$), but CXCR3$^+$ T_{FH} cells were positively correlated with neutralization titres ($r=0.486$, $P=0.012$; Fig. 3e,f). As expected, CXCR3$^-$ T_{FH} cells ($r=-0.435$, $P=0.025$) and the ratio of CXCR3$^+$/CXCR3$^-$ T_{FH} cells ($r=0.467$, $P=0.016$) were negatively and positively correlated with neutralization titres, respectively (Fig. 3g,h). These findings suggest that CXCR3$^+$ T_{FH} cells may have a dominant role in the early initiation and/or maintenance of neutralizing antibody responses in individuals who have recovered from COVID-19. The relatively high frequency of CXCR3$^+$ T_{FH}-cell subsets may contribute to the higher level of neutralizing antibody responses in the severe group compared with that in non-severe group.

To further examine whether the T_{FH} cells were SARS-CoV-2 spike specific, peripheral blood mononuclear cells (PBMCs) from COVID-19-convalescent individuals and healthy controls were stimulated with SARS-CoV-2 spike (S1 + S2) proteins or bovine serum albumin (BSA), and the antigen-specific T_{FH}-cell populations were analysed for the expression of surface marker CD154, the frequency of the OX40$^+$CD25$^+$ population, and the release of cytokines IL-21 and IFNγ (Extended Data Fig. 9a–d). As expected, CD154 expression and the CD25$^+$OX40$^+$ population were significantly increased in spike-stimulated total T_{FH} cells and CXCR3$^+$ and CXCR3$^-$ T_{FH}-cell subsets compared with BSA-stimulated controls (Fig. 3i,j). By contrast, SARS-CoV-2 spike stimulation did not significantly increase CD154 expression and the frequency of the CD25$^+$OX40$^+$ population in T_{FH} cells or their subsets of PBMCs from healthy controls (Fig. 3i,j). These results suggest that the responsive T_{FH} cells were SARS-CoV-2 spike specific. IL-21 is a signature marker cytokine of T_{FH} cells and is critical for T_{FH}-cell function[25,26]. Similarly, the release of IL-21 was significantly increased in total T_{FH} cells and T_{FH}-cell subsets after spike stimulation compared with the BSA-stimulated controls (Fig. 3k). IFNγ was produced mainly by CXCR3$^+$ T_{FH} cells after spike stimulation (Fig. 3l); for the healthy control group, a very low level of IFNγ was detected after stimulation with spike or BSA (Fig. 3l). Together, these data demonstrate that circulating T_{FH} cells in individuals who have recovered from COVID-19 are spike specific and functional—this is critical for the initiation and/or maintenance of neutralizing antibodies after SARS-CoV-2 infection.

Here, we systematically investigated neutralizing antibody responses in individuals who had recovered from COVID-19. The majority of COVID-19-convalescent individuals maintained antibodies with neutralization activity against SARS-CoV-2 (Fig. 1d), and some of these antibodies cross-neutralized SARS-CoV and/or MERS-CoV (Fig. 1f). The cross-neutralization to SARS-CoV and MERS-CoV may be explained, at least in part, by the sequence homology of spike proteins of these three coronaviruses. SARS-CoV-2 spike amino acid sequences share ~76% with SARS-CoV spike but have only ~35% identity with MERS-CoV spike[27], which may explain the finding that COVID-19 sera showed cross-neutralization more efficiently to SARS-CoV than to MERS-CoV (Fig. 1f). Neutralizing antibodies in COVID-19-convalescent individuals were reported but only for those with mild symptoms[3,15]. The cross-binding activity of COVID-19 sera was recently tested against SARS-CoV (spike and S1) and MERS-CoV spike, but included only three serum samples[28]. A report published during the revision of this manuscript also supported the finding that sera from patients who recovered from COVID-19 cross-reacted with SARS-CoV and MERS-CoV[29]. Patient-derived SARS-CoV monoclonal and receptor binding domain (RBD)-specific S309 antibodies could cross-neutralize SARS-CoV-2 (refs. [30–32]); however, a low titre of SARS-CoV serum was found without cross-neutralization for SARS-CoV-2 (ref. [16]). Indeed, with up to 67 participants, our study showed that antibody binding titres correlate positively with neutralization titres (Extended Data Fig. 4a–c), and neutralizing antibodies derived from COVID-19-convalescent individuals efficiently neutralized SARS-CoV-2 but were less efficient at neutralizing SARS-CoV and MERS-CoV (Extended Data Fig. 6c–e). It should be noted that cross-neutralization with MERS-CoV was most likely mediated by S2 binding only, as there was no detectable binding to S1 (Fig. 1c and Extended Data Fig. 3), which is consistent with recent reports[19,28]. The existence of cross-neutralizing antibodies in COVID-19-convalescent individuals provides the possibility to isolate broad neutralizing antibodies and to design pan-coronavirus vaccines.

Interestingly, individuals who recovered from severe COVID-19 elicited and maintained higher antibody and neutralization titres compared with the non-severe group (Fig. 2). Furthermore, neutralizing antibody titres were positively correlated with the severity of COVID-19 rather than other factors (Table 1 and Extended Data Fig. 1). These findings were similar to those from a report for patients who had recovered from MERS-CoV, in which the levels of neutralizing antibodies were positively associated with the number of days in ICU, viral shedding and the need for ventilation—several characteristics of critical conditions[33]. In individuals who recovered from MERS-CoV and SARS-CoV-2 infections, neutralizing antibody titres were positively correlated with antigen-specific CD4$^+$

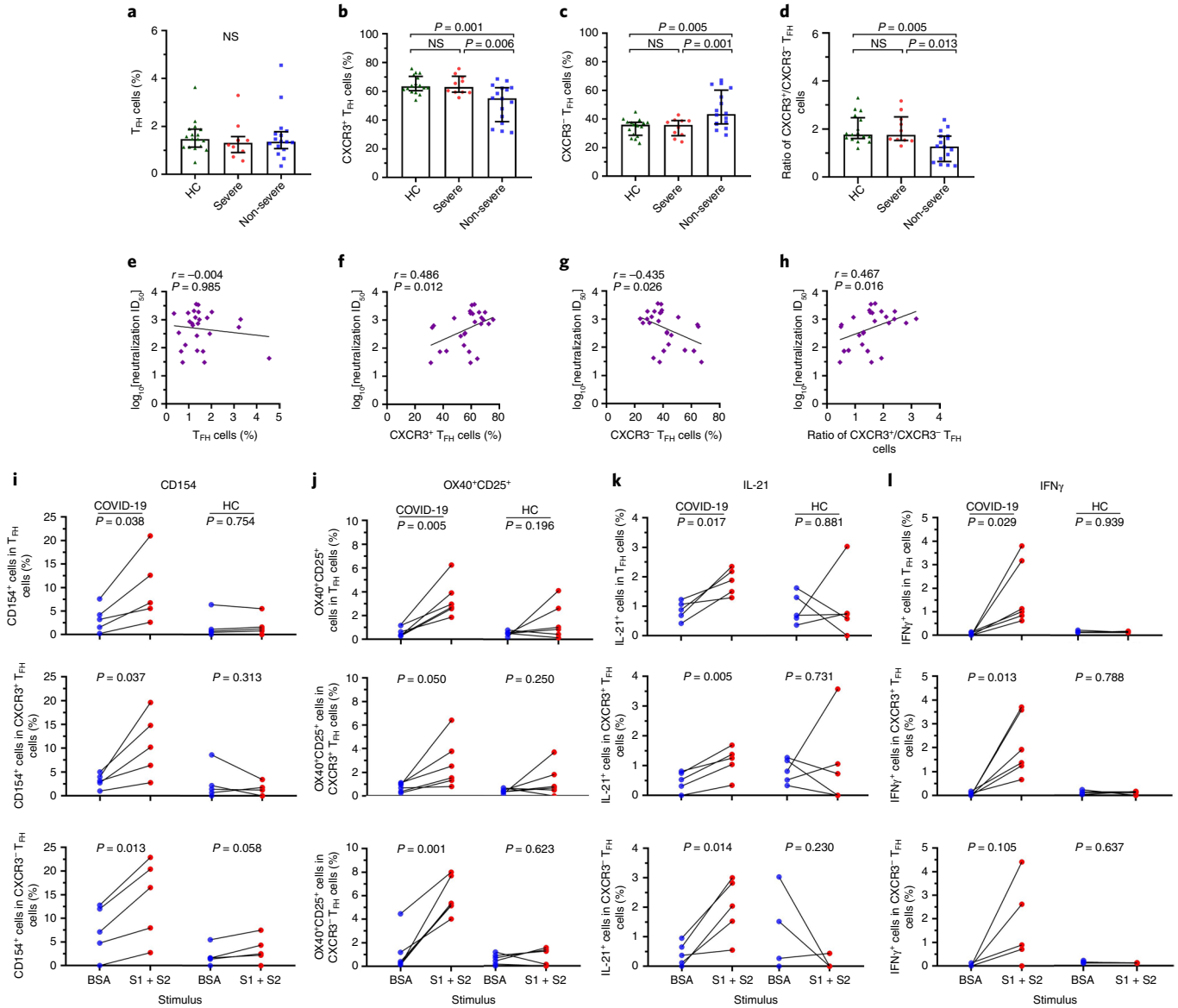

Fig. 3 | The frequency of circulating functional CXCR3$^+$ T_{FH} cells in convalescent individuals who had severe and non-severe COVID-19 is positively correlated with neutralization titres. a–d, The frequency of circulating total T_{FH} cells (**a**), CXCR3$^+$ T_{FH} cells (**b**) and CXCR3$^-$ T_{FH} cells (**c**), as well as the ratio of CXCR3$^+$/CXCR3$^-$ T_{FH} cells (**d**) in healthy controls (HC) ($n=17$), severe groups ($n=10$) and non-severe groups ($n=16$). The gating strategy for the T_{FH} cells (PD-1$^+$CXCR5$^+$CD4$^+$ T cells) is presented in Extended Data Fig. 8a, and a comparison of T_{FH}-cell subsets between healthy controls ($n=17$) and individuals who recovered from COVID-19 ($n=26$) is shown in Extended Data Fig. 8b. NS, not significant. **e–h**, Correlation analysis of the neutralization titres of antibodies and the frequencies of total T_{FH} cells (**e**), CXCR3$^+$ T_{FH} cells (**f**) and CXCR3$^-$ T_{FH} cells (**g**), as well as the neutralization titres of antibodies and the ratio of CXCR3$^+$/CXCR3$^-$ T_{FH} cells (**h**) in individuals who recovered from COVID-19 ($n=26$). Neutralization titres were $\log_{10}$-transformed. **i–l**, Spike-specific circulating T_{FH}-cell response after antigen stimulation. Spike-specific CD154$^+$ T_{FH} cells ($n=5$) (**i**) and OX40$^+$CD25$^+$ T_{FH} cells ($n=6$) (**j**), and intracellular IL-21 ($n=5$) (**k**) and IFNγ ($n=6$) (**l**) were measured using flow cytometry after stimulation. For **a–d**, data are median ± IQR (25–75%). One-way analysis of variance was used to compare the difference between multiple groups, and Tukey's multiple-comparisons test was used to compare differences within the groups. For **e–h**, Spearman's rank correlation coefficient was used to describe the association between the frequency of T_{FH}-cell subsets and the neutralization titres. For **i–l**, paired *t*-tests were used to analyse the difference in the frequency of spike-specific T_{FH}-cell subsets from COVID-19-convalescent individuals and healthy controls after stimulation. $P<0.05$ was considered to be a two-tailed significant difference.

T cells[15,33], and neutralizing antibody responses were more stable and lasted longer in those individuals who had recovered from severe symptoms of MERS-CoV infection[34]. Here, a rapid increase in lymphocyte counts in the severe COVID-19 convalescent group may be responsible for the production of the high levels of neutralizing antibodies (Fig. 2d–e). Indeed, this hypothesis is supported by the fact that a higher frequency of CXCR3$^+$ T_{FH}-cell subsets existed in the severe group compared with in non-severe group and was positively correlated with the neutralizing antibody titres (Fig. 3b–h). The correlation of CXCR3$^+$ T_{FH} cells with neutralizing antibody responses has been reported in other virus infections. Our previous study showed that, in patients with hepatitis C, CXCR3$^+$ T_{FH} cells are positively correlated with hepatitis C virus-neutralizing antibody titres and contributed to memory-B-cell activation and differentiation[35]. CXCR3$^+$ICOS$^+$CXCR5$^+$CD4$^+$ T cells[36] and circulating T-helper-1-biased helper cells[37] were also reported to be

positively correlated with influenza virus- and HIV-specific antibody responses, respectively. T_{FH} cells, as professional B helper cells, were differentiated, activated and progressively increased from day 7 after onset of SARS-CoV-2 infection[38]. Antigen stimulation substantially increased the frequency of the spike-specific $CD154^+$ and $OX40^+CD25^+$ populations, as well as IL-21- and IFNγ-releasing cells in total T_{FH} cells and $CXCR3^+$ and $CXCR3^-$ T_{FH}-cell subsets (Fig. 3i–l), which strongly supports the notion that T_{FH} cells are involved in neutralizing antibody responses in the SARS-CoV-2 infection. However, $CXCR3^+$ T_{FH} cells and $CXCR3^-$ T_{FH} cells may have different roles in antibody initiation and/or maintenance. Similar findings were published during the revision of this manuscript, in which $CCR6^+CXCR3^-$ cells were dominant spike-specific circulating T_{FH} cells that were negatively correlated with neutralizing antibody titres[39]. However, it remains unknown whether these circulating T_{FH} cells originate from germinal centres and are able to support long-lived plasma cells that are critical for the development of a SARS-CoV-2 vaccine.

Taken together, this study provides insights into the understanding of antibody responses in COVID-19-convalescent individuals and evidence facilitating the development of broad neutralizing antibodies and pan-coronavirus vaccines.

Methods

Individuals and sample collection. A total of 67 individuals who had recovered from COVID-19 were enrolled in this study, and diagnosis of COVID-19 was made according to WHO interim guidance. All patients presenting as outpatients showed fever or respiratory symptoms; chest computed tomography scans identified abnormal pulmonary nodules, and SARS-CoV-2 infection was further confirmed using quantitative PCR at the local health authority. All patients were hospitalized in the Department of Infectious Disease, The Centre Hospital of Shaoyang, Hunan Province, China, between 23 January 2020 and 2 March 2020. Patients with COVID-19 were classified into either the severe group or the non-severe group according to the Guidelines for the Diagnosis and Treatment of New Coronavirus Pneumonia (v.5) published by the National Health Commission of China. Patients were classified into the severe group once they met one of the following criteria: (1) shortness of breath with a respiratory rate ≥30 times per minute; (2) oxygen saturation (resting state) ≤93%; (3) $PaO_2/FiO_2 \leq 300$ mmHg. Otherwise, they were assigned to the non-severe group. Of the 67 patients, 17 were categorized with severe conditions and 50 had mild to moderate symptoms (referred to here as non-severe). The medical histories and the results of physical, haematological, biochemical, radiological and microbiological analyses were retrospectively evaluated and analysed. Peripheral blood of the recovered individuals was collected on day 28 after discharge, corresponding to 44–52 d after the onset of symptoms. PBMCs and serum were isolated and frozen in liquid nitrogen and in ultra-low temperature freezers, respectively.

End-point titre assay of serum antibodies. The end-point titre of serum antibodies was determined by measuring the binding activity of serum to the SARS-CoV-2 spike subunits S1 and S2 using an IgG-specific ELISA. In brief, 96-well plates (Corning) were coated with S1 or S2 at 200 ng per well in PBS at 4 °C overnight. The plates were washed five times with PBS-T (0.05% Tween-20 in PBS) and then blocked with blocking buffer (2% FBS and 2% BSA in PBS-T) for 30 min. Twofold serial dilutions of serum, starting from 1:20 dilution, were added to the 96-well plates in triplicate (100 µl per well) and incubated for 1 h at room temperature. Spike S1- and S2-specific antibodies were detected using horseradish peroxidase (HRP)-conjugated anti-human IgG and 3,3′,5,5′-tetramethylbenzidine substrate (Thermo Fisher Scientific). Sera from healthy individuals were used as negative controls, and monoclonal antibodies specific for the RBD of SARS-CoV-2 spike protein (anti-RBD/SARS-CoV-2; generated in the laboratory; unpublished data) was used as a positive control. Optical density at 450 nm (OD_{450}) was measured for each reaction, and an OD_{450} of threefold above the cutoff-OD_{450} value was considered to be a positive readout. The cross-reactivity of the serum with subunits S1 and/or S2 of either SARS-CoV or MERS-CoV spike was examined using an optimized serum dilution of 1:1,000. All antigens were His-tagged (SARS-CoV-2 spike S1 and S2; SARS-CoV spike S1 and S2; MERS-CoV spike S1 and S2) and were purchased (Sino Biological).

Avidity assay of serum antibodies. The avidity of IgG antibodies specific to SARS-CoV-2 spike S1 and S2 was measured using a modified two-step approach that was described previously[40,41]. In the first step, serum dilutions were optimized to obtain an OD_{450} value within the range of 0.5–1.5, such that it ensured a linear measurement of the antibody avidity. The second step was an ELISA, but included an elution procedure of 1 M sodium thiocyanate (NaSCN). These measurements were performed in triplicate. The avidity index of an antibody was calculated as $OD_{NaSCN\,1M}/OD_{NaSCN\,0M} \times 100\%$.

Neutralization assay of serum antibodies. The neutralization activity of serum was determined by the decrease in luciferase expression after pseudotyped virus infection of Huh7 cells, as described previously for the neutralization assay of HIV pseudotyped virus[20,21,42]. The ID_{50} was defined as the serum dilution, at which the relative light unit (RLU) value was reduced by 50% compared with the control solution wells (virus + cells). The ID_{50} values were calculated using nonlinear regression, that is, log_{10}-transformed inhibitor versus response (four parameters). In brief, SARS-CoV-2 pseudotyped virus was incubated in duplicate with the serial dilutions of sera samples (six dilutions: 1:30, 1:90, 1:270, 1:810, 1:2,430, 1:7,290) at 37 °C for 1 h. Freshly trypsinized cells were then added and incubated at 5% CO_2 and 37 °C for 24 h, and the luminescence was measured. In parallel, control wells with only virus or cells were included in six replicates. The background RLU value (cells only) was subtracted from each determination. The cross-neutralization of serum to SARS-CoV- and MERS-CoV-pseudotyped viruses was performed using similar procedures as to SARS-CoV-2-pseudotyped viruses. Healthy control sera were used as negative controls. Sera from guinea pigs immunized with the spike protein from SARS-CoV-2, SARS-CoV or MERS-CoV were used as positive controls in the neutralization experiments for SARS-CoV-2, SARS-CoV or MERS-CoV, respectively. The cut-off value was defined as $ID_{50} = 30$, and $ID_{50} > 30$ was considered to have a neutralization effect. Neutralization titres were logarithmically transformed.

Autoantibody detection. Sixteen autoimmune antibodies were tested to assess whether the autoimmunity had occurred after recovery from COVID-19. Anti-double-stranded DNA and anti-ANA antibodies were detected using ELISA (Zeus Scientific); anti-nucleosome, anti-histone, anti-SmD1, anti-U1-SnRNP, anti-SS-A/Ro 60KD, anti-SS-A/Ro 52KD, anti-SS-B/La, anti-Sc1-70, anti-CENP-B, anti-Jo-1 and anti-PO/38KD antibodies were examined using Line Immuno Assay (LIA), according to the manufacturer's protocols (HUMAN).

Flow cytometry. To analyse the circulating T_{FH} cells, cryopreserved PBMCs were thawed in a 37 °C water bath and cultured immediately in RPMI 1640 medium supplemented with 10% FBS in 5% CO_2 at 37 °C overnight. For cell-surface staining, 1×10^6 PBMCs were first labelled using the LIVE/DEAD Fixable Blue Dead Cell Stain Kit (Thermo Fisher Scientific) to distinguish live and dead cells, and then treated with Fc Block (BioLegend) to block non-specific binding. The treated PBMCs were stained with antibodies, which were pretitrated to an optimized dilution and fluorescently labelled, in 96-well V-bottom plates at 4 °C for 30 min. The fluorescently labelled antibodies used were as follows: BUV737 mouse anti-human CD4 (SK3) and PE mouse anti-human CXCR3 (1C6; BD Biosciences), FITC mouse anti-human PD-1 (EH12.2H7; BioLegend) and PE-eFluor 610 mouse anti-human CXCR5 (MU5UBEE; Thermo Fisher Scientific). Samples were loaded onto a MoFlo XDP Flow Cytometer (Beckman Coulter) immediately after antibody staining. The gating of cell populations was based on the mean fluorescence intensity minus one and unstained controls. All data were analysed using FlowJo v.10.0 (Tree Star).

Antigen-specific T_{FH}-cell assay. A CD154 assay and a cytokine-independent activation-induced marker assay (AIMs, OX40/CD25) were used to assess spike-specific (S1 and S2) circulating-T_{FH}-cell responses after stimulation[43,44]. In brief, cryopreserved PBMCs were thawed and kept resting in complete RPMI 1640 medium in 5% CO_2 at 37 °C overnight. Cells (1×10^6) were stimulated with SARS-CoV-2 spike protein (S1 + S2, 5 µg ml^{-1}) or BSA (5 µg ml^{-1}, Sigma-Aldrich) in 5% CO_2 at 37 °C for 24 h. Concanavalin A (5 µg ml^{-1}, Sigma-Aldrich) was used as a CD154 assay positive control, and staphylococcal enterotoxin B (1 µg ml^{-1}, Toxin Technology) was used as the OX40/CD25 assay positive control. PBMCs from healthy controls were also stimulated in the same conditions. Furthermore, to test the spike-specific cytokine secretion of T_{FH} cells, a conventional intracellular cytokine staining assay was used[45,46]. Intracellular secretion of IL-21 and IFNγ was measured after antigen stimulation of T_{FH} cells. In brief, PBMCs were stimulated with SARS-CoV-2 spike protein (S1 + S2, 5 µg ml^{-1}) or BSA (5 µg ml^{-1}) in the presence of anti-CD28 (1 µg ml^{-1}) and anti-CD49d (1 µg ml^{-1}) (BioLegend) antibodies for 6 h, and brefeldin A (1:1,000, BioLegend) was added 1 h after stimulation. Anti-CD3 antibodies (1 µg ml^{-1}, BioLegend) were included as a positive control. T_{FH} cells were gated as live $CD4^+PD\text{-}1^+CXCR5^+$ T cells. PE mouse anti-human CD154 (24-31), PE-Cy7 mouse anti-human OX40 (ACT35), APC-mouse anti-human IL-21 (3A3-N2), PE-Cy7 mouse anti-human IFNγ (4S.B3) (BioLegend) and PE-Cy5 mouse anti-human CD25 (M-A251) (BD Biosciences) were purchased.

Statistical analysis and reproducibility. Baseline clinical characteristics were non-normally distributed, continuous variables were expressed as median ± IQR. Rank variables were expressed as constituent ratios. Mann–Whitney *U*-tests were used to analyse two independent variables, and paired *t*-tests were used to compare two paired samples. One-way analysis of variance was used to compare the differences between multiple groups, and Tukey's multiple-comparisons test

was used to compare within the groups. χ^2 tests or Fisher's exact tests were used to analyse different distributions between groups. Spearman's rank correlation coefficient was used to measure the correlation between two different variables. A univariate and multivariable binary logistic regression model was used to rank the factors affecting the production of neutralization antibodies. OR values and 95% two-sided CIs were generalized by equation models to describe the factors contributing to antibody responses. Analyses of the data were performed using SPSS v.26 and GraphPad Prism v.8.0. Unless otherwise stated, all numeral data shown in this study were collected from at least three independent experiments. Thus, the results shown are representative of the biological replicates.

Ethics approval. This study was performed in accordance with the Good Clinical Practice and the Declaration of Helsinki principles for ethical research. The study protocol was approved by the Institutional Review Board of The Center Hospital of Shaoyang (V.1.0, 20200301), Hunan Province, China. Each participant provided informed consent by signing a written consent form. Medical data were collected from electronic records of the hospitals using standardized Data Collection Forms recommended by the International Severe Acute Respiratory and Emerging Infection Consortium.

Reporting Summary. Further information on research design is available in the Nature Research Reporting Summary linked to this article.

Data availability

Source data are provided with this paper and are available via Figshare (https://doi.org/10.6084/m9.figshare.13139423.v2). Any other data that support the findings of this study are available from the corresponding authors on request.

Received: 22 May 2020; Accepted: 29 October 2020;
Published online: 16 November 2020

References

1. Zhu, N. et al. A novel coronavirus from patients with pneumonia in China, 2019. *N. Engl. J. Med.* **382**, 727–733 (2020).
2. Zhou, P. et al. A pneumonia outbreak associated with a new coronavirus of probable bat origin. *Nature* **579**, 270–273 (2020).
3. Wu, F. et al. A new coronavirus associated with human respiratory disease in China. *Nature* **579**, 265–269 (2020).
4. Guan, W. J. et al. Clinical characteristics of coronavirus disease 2019 in China. *N. Engl. J. Med.* **382**, 1708–1720 (2020).
5. Hu, Z. et al. Clinical characteristics of 24 asymptomatic infections with COVID-19 screened among close contacts in Nanjing, China. *Sci. China Life Sci.* **63**, 706–711 (2020).
6. Wang, F. et al. Characteristics of peripheral lymphocyte subset alteration in COVID-19 pneumonia. *J. Infect. Dis.* **221**, 1762–1769 (2020).
7. Chen, G. et al. Clinical and immunological features of severe and moderate coronavirus disease 2019. *J. Clin. Invest.* **130**, 2620–2629 (2020).
8. Amanat, F. et al. A serological assay to detect SARS-CoV-2 seroconversion in humans. *Nat. Med.* **26**, 1033–1036 (2020).
9. Chen, X. et al. Human monoclonal antibodies block the binding of SARS-CoV-2 spike protein to angiotensin converting enzyme 2 receptor. *Cell Mol. Immunol.* **17**, 647–649 (2020).
10. Qin, C. et al. Dysregulation of immune response in patients with coronavirus 2019 (COVID-19) in Wuhan, China. *Clin. Infect. Dis.* **71**, 762–768 (2020).
11. Wang, F. et al. The laboratory tests and host immunity of COVID-19 patients with different severity of illness. *JCI Insight* **5**, e137799 (2020).
12. Guo, L. et al. Profiling early humoral response to diagnose novel coronavirus disease (COVID-19). *Clin. Infect. Dis.* **71**, 778–785 (2020).
13. Zhao, J. et al. Antibody responses to SARS-CoV-2 in patients of novel coronavirus disease 2019. *Clin. Infect. Dis.* https://doi.org/10.1093/cid/ciaa344 (2020).
14. Long, Q. X. et al. Antibody responses to SARS-CoV-2 in patients with COVID-19. *Nat. Med.* **26**, 845–848 (2020).
15. Ni, L. et al. Detection of SARS-CoV-2-specific humoral and cellular immunity in COVID-19 convalescent individuals. *Immunity* **52**, 971–977 (2020).
16. Anderson, D. E. et al. Lack of cross-neutralization by SARS patient sera towards SARS-CoV-2. *Emerg. Microbes Infect.* **9**, 900–902 (2020).
17. Duan, K. et al. Effectiveness of convalescent plasma therapy in severe COVID-19 patients. *Proc. Natl Acad. Sci. USA* **117**, 9490–9496 (2020).
18. Shen, C. et al. Treatment of 5 critically Ill patients with COVID-19 with convalescent plasma. *JAMA* **323**, 1582–1589 (2020).
19. Chan, K. H. et al. Cross-reactive antibodies in convalescent SARS patients' sera against the emerging novel human coronavirus EMC (2012) by both immunofluorescent and neutralizing antibody tests. *J. Infect.* **67**, 130–140 (2013).
20. Nie, J. et al. Establishment and validation of a pseudovirus neutralization assay for SARS-CoV-2. *Emerg. Microbes Infect.* **9**, 680–686 (2020).
21. Ma, J. et al. Development of SARS and MERS neutralization methods based on pseudoviruses. *Chin. J. Virol.* **35**, 189–195 (2019).
22. Breitfeld, D. et al. Follicular B helper T cells express CXC chemokine receptor 5, localize to B cell follicles, and support immunoglobulin production. *J. Exp. Med.* **192**, 1545–1552 (2000).
23. Schaerli, P. et al. CXC chemokine receptor 5 expression defines follicular homing T cells with B cell helper function. *J. Exp. Med.* **192**, 1553–1562 (2000).
24. Morita, R. et al. Human blood $CXCR5^+CD4^+$ T cells are counterparts of T follicular cells and contain specific subsets that differentially support antibody secretion. *Immunity* **34**, 108–121 (2011).
25. Nurieva, R. I. et al. Generation of T follicular helper cells is mediated by interleukin-21 but independent of T helper 1, 2, or 17 cell lineages. *Immunity* **29**, 138–149 (2008).
26. Vogelzang, A. et al. A fundamental role for interleukin-21 in the generation of T follicular helper cells. *Immunity* **29**, 127–137 (2008).
27. Grifoni, A. et al. A sequence homology and bioinformatic approach can predict candidate targets for immune responses to SARS-CoV-2. *Cell Host Microbe* **27**, 671–680 (2020).
28. Okba, N. M. A. et al. Severe acute respiratory syndrome coronavirus 2-specific antibody responses in coronavirus disease patients. *Emerg. Infect. Dis.* **26**, 1478–1488 (2020).
29. Wang, Y. et al. Kinetics of viral load and antibody response in relation to COVID-19 severity. *J. Clin. Invest.* **130**, 5235–5244 (2020).
30. Wang, C. et al. A human monoclonal antibody blocking SARS-CoV-2 infection. *Nat. Commun.* **11**, 2251 (2020).
31. Tian, X. et al. Potent binding of 2019 novel coronavirus spike protein by a SARS coronavirus-specific human monoclonal antibody. *Emerg. Microbes Infect.* **9**, 382–385 (2020).
32. Pinto, D. et al. Cross-neutralization of SARS-CoV-2 by a human monoclonal SARS-CoV antibody. *Nature* **583**, 290–295 (2020).
33. Zhao, J. et al. Recovery from the Middle East respiratory syndrome is associated with antibody and T-cell responses. *Sci. Immunol.* **2**, eaan5393 (2017).
34. Alshukairi, A. N. et al. Antibody response and disease severity in healthcare worker MERS survivors. *Emerg. Infect. Dis.* **22**, 1113–1115 (2016).
35. Zhang, J. et al. Circulating $CXCR3^+$ Tfh cells positively correlate with neutralizing antibody responses in HCV-infected patients. *Sci. Rep.* **9**, 10090 (2019).
36. Bentebibel, S. E. et al. Induction of $ICOS^+CXCR3^+CXCR5^+$ T_H cells correlates with antibody responses to influenza vaccination. *Sci. Transl. Med.* **5**, 176ra132 (2013).
37. Baiyegunhi, O. et al. Frequencies of Circulating Th1-Biased T Follicular Helper Cells in Acute HIV-1 Infection Correlate with the Development of HIV-Specific Antibody Responses and Lower Set Point Viral Load. *J. Virol.* **92**, e00659-618 (2018).
38. Thevarajan, I. et al. Breadth of concomitant immune responses prior to patient recovery: a case report of non-severe COVID-19. *Nat. Med.* **26**, 453–455 (2020).
39. Juno, J. A. et al. Humoral and circulating follicular helper T cell responses in recovered patients with COVID-19. *Nat. Med.* **26**, 1428–1434 (2020).
40. Welten, S. P. M., Redeker, A., Toes, R. E. M. & Arens, R. Viral persistence induces antibody inflation without altering antibody avidity. *J. Virol.* **90**, 4402–4411 (2016).
41. Ray, R. et al. Characterization of antibodies induced by vaccination with hepatitis C virus envelope glycoproteins. *J. Infect. Dis.* **202**, 862–866 (2010).
42. Chen, Q. et al. Development and optimization of a sensitive pseudovirus-based assay for HIV-1 neutralizing antibodies detection using A3R5 cells. *Hum. Vaccin. Immunother.* **14**, 199–208 (2018).
43. Dan, J. M. et al. A cytokine-independent approach to identify antigen-specific human germinal center T follicular helper cells and rare antigen-specific $CD4^+$ T cells in blood. *J. Immunol.* **197**, 983–993 (2016).
44. Bentebibel, S. E. et al. $ICOS^+PD\text{-}1^+CXCR3^+$ T follicular helper cells contribute to the generation of high-avidity antibodies following influenza vaccination. *Sci. Rep.* **6**, 26494 (2016).
45. Gauduin, M. C. Intracellular cytokine staining for the characterization and quantitation of antigen-specific T lymphocyte responses. *Methods* **38**, 263–273 (2006).
46. Gauduin, M. C. et al. Optimization of intracellular cytokine staining for the quantitation of antigen-specific $CD4^+$ T cell responses in rhesus macaques. *J. Immunol. Methods* **288**, 61–79 (2004).

Acknowledgements

We thank all of the participants. This work was supported by the COVID-19 Emergency Special Program of Hunan Province (no. 2020SK3052, to W. Liu), Key Research and Development Project of Chenzhou City, Hunan Province (no. ZDYF2020010 and ZDYF2020007) and by the SC1-PHE-CORONAVIRUS-2020: Advancing knowledge for the clinical and public health response to the 2019-nCoV epidemic' from the European Commission (CORONADX, no. 101003562, to Y.-P.L.).

Author contributions

X. Qu, W. Liu, Y.-P.L. and Y.W. contributed to the study design and data interpretation. Q. Wang, T.X., M.H., D.P., G.L., X.X., S.H., Y.D., J.L., W. Li, Z. Lu, H.C., T.Z. and Q.L. contributed to clinical management, patient recruitment and data collection. J.Z., Q. Wu, Z. Liu, J.W., Y.H., T.B., T.W., W.H., K.J., L.N., W.G., D. Luo and Y.-P.L. contributed to sample processing, assay development and performing experiments. J.Z., Q. Wu, Z. Liu, T.W., D. Lei and R.H. contributed to statistical analysis and data visualization. X. Qu, W. Liu, Y.-P.L. and J.Z. drafted the manuscript. Y.W., X. Qu and Y.-P.L. contributed to revision of the manuscript for important intellectual content. X. Qu and W. Liu provided supervision. All of the authors met authorship criteria and approved the publication.

Competing interests

The authors declare no competing interests.

Additional information

Extended data is available for this paper at https://doi.org/10.1038/s41564-020-00824-5.

Supplementary information is available for this paper at https://doi.org/10.1038/s41564-020-00824-5.

Correspondence and requests for materials should be addressed to Y.-P.L., Y.W., W.L. or X.Q.

Peer review information: *Nature Microbiology* thanks the anonymous reviewers for their contribution to the peer review of this work.

Reprints and permissions information is available at www.nature.com/reprints.

Publisher's note Springer Nature remains neutral with regard to jurisdictional claims in published maps and institutional affiliations.

	Total (n=67)	Severe group (n=17)	Non-severe group (n=50)	*p* value
Basic information				
Age (years) (IQR)	43(30-53)	59(45-69.5)	41(29-47)	<0.0001*
Sex				
Male	34(50.8)	11(64.7)	23(46)	0.26
Female	33(49.3)	6(35.3)	27(54)	
Course of disease (days) (IQR)	20(16-25)	25(21-28)	18(16-23.3)	0.007*
Presenting symptoms and signs				
Cough	59(88.1)	17(100)	42(84)	0.10
Fever	58(86.6)	17(100)	41(82)	0.10
Fatigue	41(61.2)	12(70.6)	29(58)	0.40
Expectoration	28(41.8)	12(70.6)	16(32)	0.009*
Dyspnea	26(38.8)	15(88.2)	11(22)	<0.0001*
Myalgia	26(38.8)	6(35.3)	20(40)	0.78
Chills	21(31.3)	12(70.6)	9(18)	<0.0001*
Headache	16(23.9)	5(29.4)	11(22)	0.53
Anhelation	10(14.9)	5(29.4)	5(10)	0.11
Diarrhea	5(7.5)	2(11.8)	3(6)	0.60
Maximum body temperature (°C) (IQR)	38.3(37.7-38.7)	38.5(38-39.1)	38.3(37.5-38.5)	0.054
SaO_2 (IQR)	98(97-99)	97(95-98.5)	99(97-99)	0.010*
PO_2 (IQR)	101(87-138)	89(74-106.5)	109.5(91.75-139.25)	0.009*
P(a/A) O_2 (IQR)	1.02(0.85-1.37)	0.84(0.73-1.02)	1.09(0.94-1.49)	0.002*
P(A-a) O_2 (IQR)	100(95-105)	102(100.5-106)	99(94.5-103.5)	0.022*
Underlying disease				
Cardiovascular diseases	16(23.9)	9(52.9)	7(14)	0.002*
Hypertension	13(19.4)	8(47.1)	5(10)	0.002*
Diabetes	9(13.4)	6(35.3)	3(6)	0.006*
COPD	4(6)	3(17.7)	1(2)	0.047*
HBV	3(4.5)	1(5.9)	2(4)	>0.999
Total underlying disease	24(35.8)	13(76.5)	11(22)	<0.0001*
Comorbidities				
Liver insufficiency	29(43.3)	13(76.5)	16(32)	0.002*
Cardiac insufficiency	25(37.3)	9(52.9)	16(32)	0.15
Renal insufficiency	4(6)	2(11.8)	2(4)	0.27
Total Comorbidities	40(59.7)	14(82.4)	26(52)	0.044*
Treatments				
Interferon inhalation	60(89.6)	15(88.2)	45(90)	>0.999
Oxygen treatment	59(88.1)	17(100)	42(84)	0.10
Antiviral treatment	58(86.6)	14(82.4)	44(88)	0.68
Traditional Chinese medicine	50(74.6)	12(70.6)	38(76)	0.75
Antibiotic treatment	31(46.3)	17(100)	14(28)	<0.0001*
Hormone therapy	15(22.4)	10(58.8)	5(10)	0.0001*
Intravenous immunoglobulin therapy	12(17.9)	7(41.2)	5(10)	0.008*
Mechanical Ventilation	5(7.5)	5(29.4)	0	ND

Extended Data Fig. 1 | Baseline characteristics of COVID-19 patients included in this study. Data of continuous variable are expressed as median (Interquartile range, IQR), rank variables are expressed as positive cases (percentage). Mann-Whitney U test was used to continuous variable companion analysis, χ^2 or Fisher's exact tests was used to rank variables data analysis. *$p < 0.05$ was considered to be a two-tailed significant difference between severe and non-severe groups.

	Normal range	Total (n=67)	Severe group (n=17)	Non-severe group (n=50)	*p* value
Blood routine					
White blood cell count ($\times10^9\,l^{-1}$)	4-10	5.4(4.2-8.7)	5.4(4.1-11.3)	5.4(4.1-8.1)	0.41
Red blood cell count ($\times10^9\,l^{-1}$)	3.5-5	4.7(4.2-5.1)	4.7(4.1-5.2)	4.8(4.2-5.1)	0.54
Neutrophil count ($\times10^9 l^{-1}$)	1.4-7	3.7(2.5-6.9)	4.7(2.7-8.7)	3.7(2.3-5.9)	0.08
Neutrophil percentage (%)	45-75	66(56.9-77)	63.9(60.2-76.4)	66.5(55.9-77.4)	0.83
Lymphocyte count ($\times10^9 l^{-1}$)	1.2-3.5	1(0.7-1.7)	0.7(0.4-0.9)	1.2(0.9-1.8)	<0.0001*
Lymphocyte percentage (%)	20-40	23(14.1-31.7)	24.9(13.5-28.3)	22.6(14.5-33.9)	0.67
Monocyte count ($\times10^9\,l^{-1}$)	0.1-1.2	0.53(0.38-0.63)	0.49(0.29-0.66)	0.54(0.39-0.62)	0.92
Monocyte percentage (%)	3-12	8.5(6.5-11.1)	8.9(6.9-12.3)	8.4(6.5-10.9)	0.35
Platelet count ($\times10^9\,l^{-1}$)	125-350	223(154-258)	154(133-191)	234.5(187-270.8)	0.001*
Hemoglobin ($g\,l^{-1}$)	120-160	142(126-153)	137(122-150.5)	142.5(126-157)	0.45
Hematocrit (%)	35-51	40.1(36.2-44.9)	38.1(36.1-43.5)	41(36.1-45.4)	0.24
Basophil percentage (%)	0-1	0.11(0-0.5)	0.12(0-0.5)	0.11(0-0.5)	0.93
Basophil count ($\times10^9\,l^{-1}$)	0.12-0.8	0.01(0-0.04)	0.01(0-0.03)	0.01(0-0.04)	0.64
Eosinophil percentage (%)	0.5-5	0.5(0-3.2)	0.4(0-1.7)	0.5(0-3.2)	0.78
Eosinophil count ($\times10^9\,l^{-1}$)	0.05-0.3	0.03(0-0.17)	0.02(0-0.08)	0.03(0-0.17)	0.66
Blood biochemistry					
Albumin ($g\,l^{-1}$)	40-55	40.4(36.1-43.5)	36.1(33.5-38.6)	41.7(38.3-45.2)	<0.0001*
Total protein ($g\,l^{-1}$)	62-85	68(64-72.6)	67.8(63-73.7)	68.3(64.2-72.6)	0.86
Creatinine ($\mu mol\,l^{-1}$)	40-88	62.7(52.3-80.2)	80.2(63.6-86.4)	61.2(46.7-77.1)	0.007*
Creatine kinase ($U\,l^{-1}$)	25-190	70.5(50.8-112.8)	102(49-169.3)	68(51.2-96.6)	0.08
Creatine kinase-MB ($U\,l^{-1}$)	0-24	15(12.4-20)	15.5(13-23)	15(11.9-19.3)	0.45
Lactate dehydrogenase ($U\,l^{-1}$)	109-245	238.5(192.1-316.3)	316(266.5-412.2)	225.1(184.8-289.8)	0.0001*
Alanine aminotransferase ($U\,l^{-1}$)	8-45	21(14-37)	28.8(15.4-48.1)	18.9(13.6-35.3)	0.31
Aspartate aminotransferase ($U\,l^{-1}$)	14-38	27(21.3-35)	31.5(25.2-50.3)	25.6(20.2-32.1)	0.019*
Total bilirubin ($mmol\,l^{-1}$)	2-20.4	12.3(8.1-20.3)	15.9(10-22.2)	12(7.2-19.9)	0.31
Total bile acid ($\mu mol\,l^{-1}$)	0-10	4.5(1.9-7.8)	4.5(2.2-8.1)	4.1(1.7-7.6)	0.42
Total cholesterol ($mmol\,l^{-1}$)	0-5.2	3.7(3.1-4.4)	3.3(2.9-4)	3.8(3.2-4.4)	0.08
Urea ($mmol\,l^{-1}$)	2-8.3	4(3.3-4.9)	4.6(3.7-5.8)	3.9(3.1-4.6)	0.07
Uric acid ($\mu mol\,l^{-1}$)	150-450	249.4(177.2-33)	208.2(155.3-284.5)	254.8(186.2-332.9)	0.10
Potassium ($mmol\,l^{-1}$)	3.5-5.3	3.8(3.5-4.1)	3.6(3.4-4)	3.9(3.6-4.2)	0.09
Sodium ($mmol\,l^{-1}$)	137-147	141.4(138.4-144.5)	137.1(134.8-142.7)	142(139.2-145)	0.016*
Glucose ($mmol\,l^{-1}$)	3.9-6.1	7.1(5.7-9.9)	9.4(7.7-14.3)	6.3(5.5-8.5)	0.0001*
Myoglobin ($\mu g\,l^{-1}$)	0-90	57.4(48.3-71.2)	58.8(51.7-72.2)	57.3(47.2-70.9)	0.81
Alkaline phosphatase ($U\,l^{-1}$)	35-125	49.4(37.7-76.1)	86.3(56.4-172.1)	43.2(35.1-61.3)	0.80
β2microglobulin ($mg\,l^{-1}$)	1-3	2.7(2.1-3.8)	3.2(2.5-4.1)	2.6(2-3.6)	0.06
Procalcitonin ($ng\,ml^{-1}$)	0-0.05	0.03(0-0.05)	0.04(0.02-0.09)	0.03(0-0.05)	0.031*
Erythrocyte sedimentation rate ($mm\,h^{-1}$)	0-15	42(18.5-80.5)	73(22.6-93.7)	39(16-56)	0.12
Coagulation function					
Prothrombin time (s)	8-14	11.1(10.4-12)	11.3(10.5-12)	11(10.3-12.1)	0.35
Thrombin time (s)	14-21	17.3(16.4-17.8)	16.6(16.2-17.7)	17.3(16.5-18)	0.65
Activated partial thromboplastin time (s)	20-40	30.2(26.3-37)	33.5(30.1-39.7)	29(23.1-36.7)	0.117
D-dimer ($mg\,l^{-1}$)	0-0.55	0.29(0.16-0.47)	0.48(0.28-0.7)	0.21(0.16-0.43)	0.003*

Extended Data Fig. 2 | Laboratory findings of COVID-19 patients on admission. Data were collected on admission and presented as median, IQR (25%-75%). Mann-Whitney U test was used to analysis of difference between two groups. *$p < 0.05$ was considered to be a two-tailed significant difference.

Patient ID	Endpoint titer to SARS-CoV-2		Avidity index (%) for SARS-CoV-2		Cross-binding SARS-CoV		Cross-binding MERS- CoV		Neutralization (ID_{50})		
	S1	S2	S1	S2	S1	S2	S1	S2	SARS-CoV-2	SARS-CoV	MERS-CoV
Severe group (n=17)											
PT1	14960	81920	44	48	+	+	-	+	735	<30	<30
PT2	40960	655360	28	80	+	+	-	+	728	253	<30
PT3	40960	327680	22	46	+	+	-	+	2067	<30	35
PT4	40960	40960	54	63	+	+	-	+	1037	406	<30
PT5	40960	81920	59	63	+	+	-	+	686	<30	68
PT6	81920	327680	57	67	+	+	-	+	3397	476	<30
PT7	40960	327680	29	29	+	+	-	+	1750	73	<30
PT8	81920	327680	57	60	+	+	-	-	1316	518	<30
PT9	81920	655360	58	61	+	+	-	-	1625	98	<30
PT10	81920	163840	41	72	-	+	-	+	1881	328	<30
PT11	320	320	NA	NA	-	-	-	-	<30	<30	<30
PT12	40960	327680	21	66	-	+	-	+	3457	513	<30
PT13	81920	655360	26	60	-	+	-	+	1225	76	54
PT14	20480	327680	34	49	-	+	-	+	1898	30	<30
PT15	20480	40960	55	49	-	+	-	+	403	426	<30
PT16	40960	327680	30	29	-	+	-	+	495	249	<30
PT17	81920	327680	37	64	-	+	-	+	1149	149	35
Non-severe group (n=50)											
PT18	20480	81920	37	70	+	+	-	+	218	409	<30
PT19	81920	81920	47	66	+	+	-	+	631	209	<30
PT20	40960	327680	44	77	+	+	-	+	859	160	<30
PT21	81920	81920	47	62	+	+	-	+	722	<30	<30
PT22	81920	81920	52	58	+	+	-	+	585	423	53
PT23	81920	655360	40	41	+	+	-	+	1006	398	<30
PT24	40960	40960	49	53	+	+	-	+	1673	133	<30
PT25	40960	20480	27	39	+	+	-	-	558	191	<30
PT26	81920	655360	37	49	+	+	-	-	3615	483	<30
PT27	20480	81920	40	55	+	+	-	+	1168	<30	<30
PT28	20480	81920	45	41	+	+	-	+	1214	<30	<30
PT29	20480	655360	26	70	+	+	-	+	269	<30	61
PT30	40960	163840	48	62	+	+	-	+	815	<30	49
PT31	81920	327680	47	55	+	+	-	+	576	376	<30
PT32	81920	327680	49	47	+	+	-	+	1395	141	<30
PT33	40960	327680	23	55	+	+	-	+	956	159	<30
PT34	40960	327680	15	58	+	+	-	+	2941	86	<30
PT35	20480	40960	52	68	-	+	-	+	100	70	<30
PT36	10240	81920	39	55	-	+	-	-	75	394	<30
PT37	2560	81920	66	90	-	+	-	+	332	486	<30
PT37	2560	81920	66	90	-	+	-	+	332	486	<30
PT38	1280	5120	42	69	-	-	-	-	<30	<30	<30
PT39	5120	655360	58	95	-	+	-	+	344	136	<30
PT40	10240	20480	52	69	-	+	-	+	316	68	<30
PT41	20480	20480	32	49	-	+	-	-	90	380	<30
PT42	10240	81920	46	67	-	+	-	+	544	<30	<30
PT43	320	320	NA	NA	-	-	-	-	79	<30	<30
PT44	10240	40960	41	41	-	+	-	+	255	99	36
PT45	20480	81920	49	73	-	+	-	+	546	390	<30
PT46	40960	81920	48	55	-	+	-	+	282	39	<30
PT47	2560	81920	54	79	-	+	-	+	125	337	<30
PT48	320	320	NA	NA	-	-	-	+	42	309	<30
PT49	20480	40960	34	57	-	-	-	+	215	<30	<30
PT50	40960	81920	23	52	-	+	-	-	1395	169	<30
PT51	40960	327680	39	57	-	+	-	+	211	185	<30
PT52	40960	81920	41	52	-	+	-	+	813	<30	67
PT53	10240	81920	49	67	-	+	-	-	249	77	<30
PT54	40960	81920	51	42	-	+	-	-	452	<30	<30
PT55	40960	163840	27	44	-	+	-	+	540	188	<30
PT56	40960	327680	23	37	-	+	-	+	1433	420	272
PT57	2560	40960	49	51	-	+	-	+	395	248	34
PT58	5120	20480	56	61	-	-	-	-	113	440	<30
PT59	10240	163840	56	53	-	+	-	+	1389	416	<30
PT60	5120	5120	66	65	-	-	-	-	92	<30	<30
PT61	81920	81920	43	67	-	+	-	-	837	420	<30
PT62	10240	81920	56	62	-	+	-	+	335	47	<30
PT63	5120	81920	42	44	-	+	-	+	184	62	<30
PT64	5120	40960	48	71	-	+	-	-	139	44	<30
PT65	10240	81920	36	47	-	+	-	+	88	59	<30
PT66	10240	81920	50	66	-	+	-	-	151	54	<30
PT67	10240	40960	46	50	-	+	-	-	436	101	38
Healthy control(n=10)											
HC1	ND	ND	NA	NA	-	-	-	-	<30	<30	<30
HC2	ND	ND	NA	NA	-	-	-	-	<30	<30	<30
HC3	ND	ND	NA	NA	-	-	-	-	<30	<30	<30
HC4	ND	ND	NA	NA	-	-	-	-	<30	<30	<30
HC5	ND	ND	NA	NA	-	-	-	-	<30	<30	<30
HC6	ND	ND	NA	NA	-	-	-	-	<30	<30	<30
HC7	ND	ND	NA	NA	-	-	-	-	<30	<30	<30
HC8	ND	ND	NA	NA	-	-	-	-	<30	<30	<30
HC9	ND	ND	NA	NA	-	-	-	-	<30	<30	<30
HC10	ND	ND	NA	NA	-	-	-	-	<30	<30	<30

Extended Data Fig. 3 | See next page for caption.

Extended Data Fig. 3 | Reactivity of anti-SARS-CoV-2 antibody to the spike subunits S1 and S2 and neutralization to SARS-CoV-2, SARS-CoV, and MERS-CoV viruses. Antibody binding titers to S1 and S2 of SARS-CoV-2 spike were performed by endpoint dilution assay and expressed as endpoint dilution titers. The avidity of antibody is expressed as avidity index (%). Cross-binding to spike S1 and S2 from both SARS-CoV and MERS-CoV were expressed as (+) (with binding) and (-) (without binding). Neutralization to SARS-CoV-2 and cross-neutralization to SARS-CoV or MERS-CoV were expressed as ID_{50}, and $ID_{50} > 30$ was defined as positive, according to the cutoff value of neutralization assay. ND, not detectable; NA, no applicable. See Methods for the details of each assay.

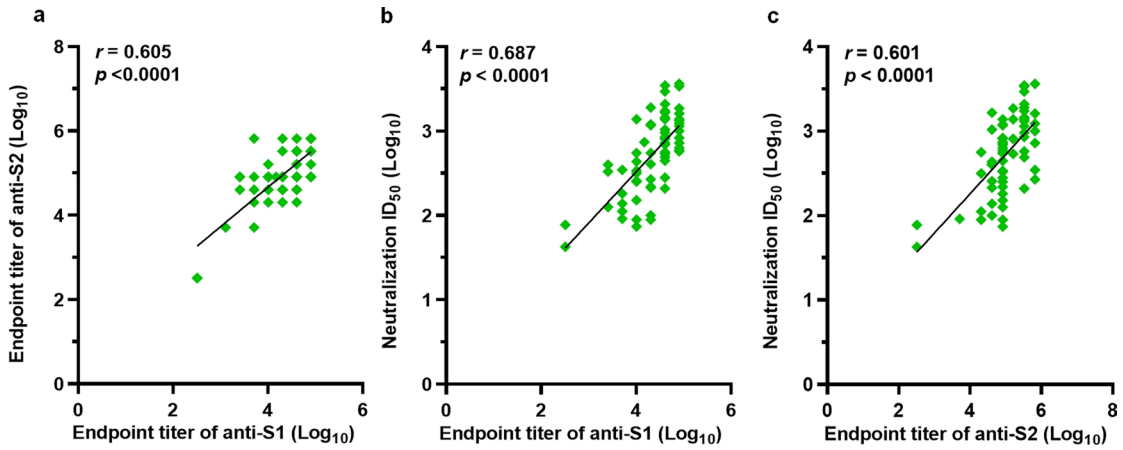

Extended Data Fig. 4 | Correlation analysis of the neutralization titers and the endpoint titers of anti-S1 and anti-S2 antibodies. Correlation analysis of endpoint titers of anti-S1 and anti-S2 antibodies (**a**) (n = 67), neutralization titers and anti-S1 titers (**b**) (n = 65), and neutralization titers and anti-S2 titers (**c**) (n = 65). Endpoint titers and neutralization titers are log_{10}-transformed. Spearman's rank coefficient of correlation was used for the correlation analysis, and $p < 0.05$ was considered to be significant difference.

Healthy control	SARS-CoV-2		SARS-CoV		MERS-CoV	
serum	S1	S2	S1	S2	S1	S2
HC11	-	-	-	-	-	-
HC12	-	-	-	-	-	-
HC13	-	-	-	-	-	-
HC14	-	-	-	-	-	-
HC15	-	-	-	-	-	-
HC16	-	-	-	-	+	-
HC17	-	-	-	-	-	-
HC18	-	-	-	-	-	-
HC19	-	-	-	-	-	-
HC20	-	-	-	-	-	-
HC21	-	-	-	-	-	-
HC22	-	-	-	-	-	-
HC23	-	-	-	-	-	-
HC24	-	-	-	-	-	-
HC25	-	-	-	-	-	-
HC26	-	-	-	-	-	-
HC27	-	-	-	-	-	-
HC28	-	-	-	-	-	-
HC29	-	-	-	-	-	-
HC30	-	-	-	-	-	-
HC31	-	-	-	-	-	-
HC32	-	-	-	-	-	-
HC33	-	-	-	-	-	-
HC34	-	-	-	-	-	-
HC35	-	-	-	-	-	-
HC36	-	-	-	-	-	-
HC37	-	-	-	-	-	-
HC38	-	-	-	-	-	-
HC39	-	-	-	-	-	-
HC40	-	-	-	-	-	-
HC41	-	-	-	-	-	-
HC42	-	-	-	-	-	-
HC43	-	-	-	-	-	-
HC44	-	-	-	-	-	-
HC45	-	-	-	-	-	-
HC46	-	-	-	-	-	-
HC47	-	-	-	-	-	-
HC48	-	-	-	-	-	-
HC49	-	-	-	-	-	-
HC50	-	-	-	-	-	-
HC51	-	-	-	-	-	-
HC52	-	-	-	-	-	-
HC53	-	-	-	+	-	-
HC54	-	-	-	-	-	+
HC55	-	-	-	-	-	-
HC56	-	-	-	-	-	-
HC57	-	-	-	-	-	-
HC58	-	-	-	-	-	-
HC59	-	-	-	-	-	-
HC60	-	-	-	-	-	-
HC61	-	-	-	-	-	-
HC62	-	-	-	-	-	-
HC63	-	-	-	-	+	-
HC64	-	-	-	-	-	-
HC65	-	-	-	-	+	-
HC66	-	-	-	-	+	-
HC67	-	-	-	-	-	-
HC68	-	-	-	-	-	-
HC69	-	-	-	-	-	-
HC70	-	-	-	-	-	-
HC71	+	-	-	-	-	-

Extended Data Fig. 5 | Binding analysis of healthy control sera against spike S1 and S2 from SARS-CoV-2, SARS-CoV, and MERS-CoV. Sixty-one healthy control sera were examined for its binding to the spike S1 and S2 from SARS-CoV-2, SARS-CoV, and MERS-CoV. The binding activity is expressed as (+) (with binding) and (-) (without binding). See Methods for the details of the assay.

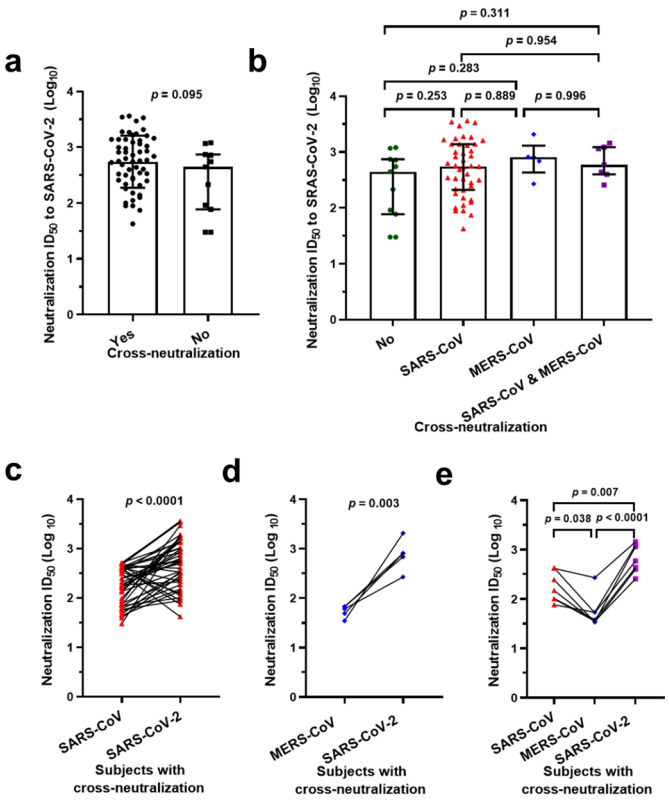

Extended Data Fig. 6 | Analysis of neutralization titers for the sera with cross-neutralization activity. a, Neutralization titers to SARS-CoV-2 pseudotyped virus for the sera with (n = 56) and without (n = 11) cross-neutralization activity to SARS-CoV and/or MERS-CoV. **b**, Comparison of neutralization titers to SARS-CoV-2 (n = 11) for the sera without cross-neutralization and with cross-neutralization to SARS-CoV (n = 44), MERS-CoV (n = 5), and both viruses (n = 7). **c**-**e**, Comparison of neutralization titer (specific and cross neutralization) for each serum that shows cross-neutralization activity. **c**, Neutralization titers to SARS-CoV and SARS-CoV-2 for those sera cross-neutralizing SARS-CoV (n = 44). **d**, Neutralization titers to MERS-CoV and SARS-CoV-2 for those sera cross-neutralizing MERS-CoV (n = 5). **e**, Neutralization titers to SARS-CoV, MERS-CoV, and SARS-CoV-2 for those sera cross-neutralizing both SARS-CoV and MERS-CoV (n = 7). Neutralization titers are log_{10}-transformed. In **a** and **b**, data presented as median, interquartile range (25%-75%). Mann-Whitney U test is used to compare the difference between two groups (**a**). One-way ANOVA is used to compare the difference among multi-groups, and Tukey's multiple comparisons test is used for intra-groups (**b**). In **c**-**e**, paired t test is used to analysis the difference between groups. $p < 0.05$ was considered to be significant difference between the groups.

Patient ID	ANA titer	Anti-ds-DNA (IU/ml)	Nucleosomes	Histones	SmD1	U1-SnRNP	SS-A/Ro (60 kDa)	SS-A/Ro (52 kDa)	SS-B/La	Scl-70	CENP-B	Jo-1	Anti-P0 (38 kDa)
PT1	1:20	28	-	-	-	-	+	-	-	-	-	-	-
PT2	<1:20	38	-	-	+	-	-	-	-	-	-	-	-
PT3	<1:20	27	-	-	-	-	-	-	-	-	-	-	-
PT4	<1:20	103	-	-	-	-	-	-	-	-	-	-	-
PT5	<1:20	35	-	-	-	-	-	-	+	-	-	-	-
PT6	<1:20	64	-	-	-	-	+	-	-	-	-	-	-
PT7	<1:20	17	-	-	-	-	-	-	-	-	-	-	-
PT8	<1:20	54	-	-	-	-	-	-	-	-	-	-	-
PT9	<1:20	43	-	-	-	-	-	-	-	-	-	-	-
PT10	<1:20	24	-	-	-	-	-	-	-	-	-	-	-
PT11	<1:20	55	-	-	-	-	-	-	-	-	-	-	-
PT12	1:20	37	-	-	-	-	-	-	-	-	-	-	-
PT13	<1:20	88	-	-	-	-	-	-	+	-	-	-	-
PT14	<1:20	206	-	-	-	-	-	-	-	-	-	-	-
PT15	<1:20	31	-	-	-	-	-	-	-	-	-	-	-
PT16	<1:20	170	-	-	-	-	-	-	-	-	-	-	-
PT17	<1:20	23	-	-	-	-	-	-	-	-	-	-	-
PT18	<1:20	64	-	-	-	-	-	-	+	-	-	-	-
PT19	<1:20	35	-	-	-	-	-	-	-	-	-	-	-
PT20	<1:20	84	-	-	-	-	-	-	-	-	-	-	-
PT21	<1:20	50	-	-	-	-	-	-	-	-	-	-	-
PT22	<1:20	36	-	-	-	-	-	-	-	-	-	-	-
PT23	<1:20	46	-	-	-	-	-	-	-	-	-	-	-
PT24	<1:20	15	-	-	-	-	-	-	-	-	-	-	-
PT25	1:40	28	-	-	-	-	-	-	-	-	-	-	-
PT26	<1:20	40	-	-	-	-	-	-	-	-	-	-	-
PT27	<1:20	43	-	-	-	-	-	-	-	+	-	-	-
PT28	<1:20	33	-	-	-	-	-	-	-	-	-	-	-
PT29	<1:20	39	-	-	-	-	-	-	-	-	-	-	-
PT30	<1:20	44	-	-	-	-	-	-	-	-	-	-	-
PT31	1:20	63	-	-	-	-	-	-	-	-	-	-	-
PT32	<1:20	51	-	-	-	-	-	-	-	-	-	-	-
PT33	<1:20	30	-	-	-	-	-	-	-	-	-	-	-
PT34	1:80	51	-	-	-	-	+	-	-	-	-	-	-
PT35	<1:20	25	-	-	-	-	-	-	-	-	-	-	-
PT36	<1:20	52	-	-	-	-	-	-	-	-	-	-	-
PT37	<1:20	46	-	-	-	-	-	-	-	-	-	-	-
PT38	<1:20	19	-	-	-	-	-	-	-	-	-	-	-
PT39	<1:20	35	-	-	+	-	-	-	-	-	-	-	-
PT40	<1:20	30	-	-	-	-	-	-	-	-	-	-	-
PT41	<1:20	17	-	-	-	-	-	-	-	-	-	-	-
PT42	<1:20	98	-	-	-	-	-	-	-	-	-	-	-
PT43	<1:20	15	-	-	-	-	+	-	+	-	-	-	-
PT44	<1:20	152	-	-	-	-	-	-	-	-	-	-	-
PT45	<1:20	28	-	-	-	-	-	-	-	-	-	-	-
PT46	<1:20	22	-	-	-	-	-	-	-	-	-	-	-
PT47	<1:20	24	-	-	-	-	-	-	-	-	-	-	-
PT48	<1:20	58	-	-	-	-	-	-	-	-	-	-	-
PT49	<1:20	37	-	-	-	-	-	-	-	-	-	-	-
PT50	<1:20	43	-	-	-	-	-	-	-	-	-	-	-
PT51	1:80	50	-	-	-	-	+	-	-	-	-	-	-
PT52	1:20	15	-	-	-	-	-	-	-	-	-	-	-
PT53	<1:20	37	-	-	-	-	-	-	-	-	-	-	-
PT54	<1:20	81	-	-	-	+	-	-	-	-	-	-	-
PT55	<1:20	34	-	-	-	-	-	-	-	-	-	-	-
PT56	<1:20	24	-	-	-	-	-	-	-	-	-	-	-
PT57	<1:20	43	-	-	-	-	-	-	-	-	-	-	-
PT58	<1:20	28	-	-	-	-	-	-	-	-	-	-	-
PT59	<1:20	30	-	-	-	-	-	-	-	-	-	-	-
PT60	<1:20	32	-	-	-	+	-	-	-	-	-	-	-
PT61	<1:20	41	-	-	-	-	-	-	-	-	-	-	-
PT62	<1:20	41	-	-	-	-	-	-	-	-	-	-	-
PT63	<1:20	31	-	-	-	-	-	-	-	-	-	-	-
PT64	<1:20	201	-	-	-	-	-	-	-	-	-	-	-
PT65	<1:20	46	-	-	-	-	-	-	-	-	-	-	-
PT66	<1:20	54	-	-	-	-	-	-	-	-	-	-	-
PT67	<1:20	39	-	-	-	-	-	-	-	-	-	-	-

Extended Data Fig. 7 | See next page for caption.

Extended Data Fig. 7 | Analysis of autoimmune antibodies in recovered COVID-19 individuals. ANA: Antinuclear antibodies; Anti-ds-DNA: Anti-double-stranded DNA; SmD1: Core small nuclear ribonucleoprotein particle splicing factor; SS-A/Ro: Anti-Sjogren's Syndrome antigen B antibody; SS-B/La: Anti-Sjogren's Syndrome B antibody; Scl-70: Autoantibodies to topoisomerase I; CENP-B: The major human centromere autoantigen; Jo-1: Histidyl-transfer RNA synthetase; Anti-P0: Anti-P antibodies react against acidic phosphorylated ribosomal proteins P0, P1, and P2 (with molecular mass of 38, 19, and 17 kDa, respectively). ANA titer≥20 and Anti-ds-DNA ≥ 180 are defined as positive (+) or less are negative (-).

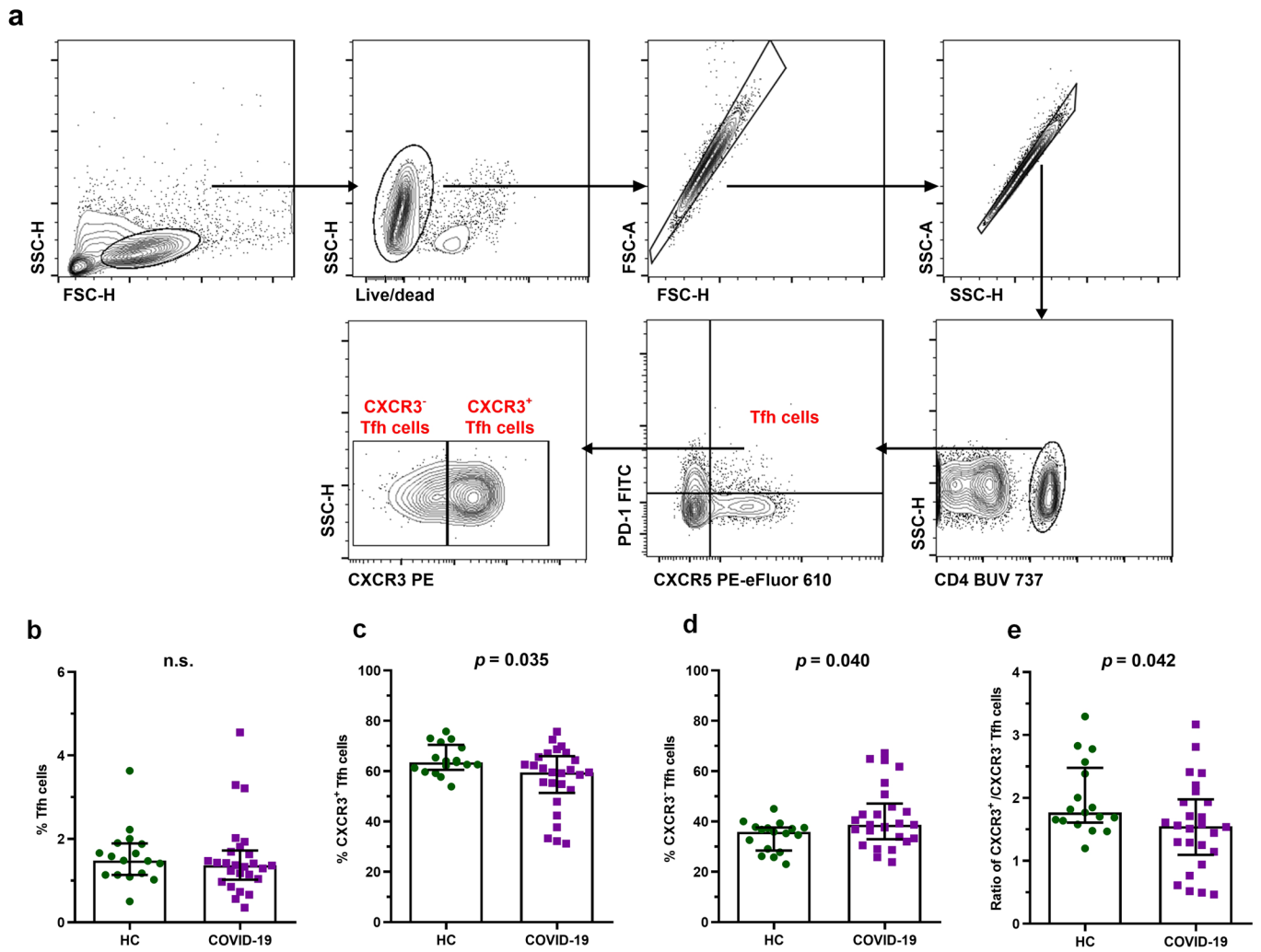

Extended Data Fig. 8 | The gating strategy and the frequency of circulating Tfh cell subsets in recovered COVID-19 individuals. a, Representative gating strategy for circulating Tfh (PD-1$^+$CXCR5$^+$ CD4$^+$ T) cells, CXCR3$^+$ and CXCR3$^-$ Tfh cells. Gating of cell populations is based on the mean fluorescence intensity 'minus one' (FMO). **b**-**e**, Comparison of between healthy controls (HC) (n = 17) percentage of Tfh cells (**b**), CXCR3$^+$ Tfh cells (**c**), CXCR3$^-$ Tfh cells (**d**), and the ratio of CXCR3$^+$/CXCR3$^-$ Tfh cells (**e**) and recovered COVID-19 individuals (n = 26). In **b**-**e**, data presented as median, interquartile range (25%-75%). Mann-Whitney U test was used to compare the difference between two groups, and $p < 0.05$ was considered to be a two-tailed significant difference.

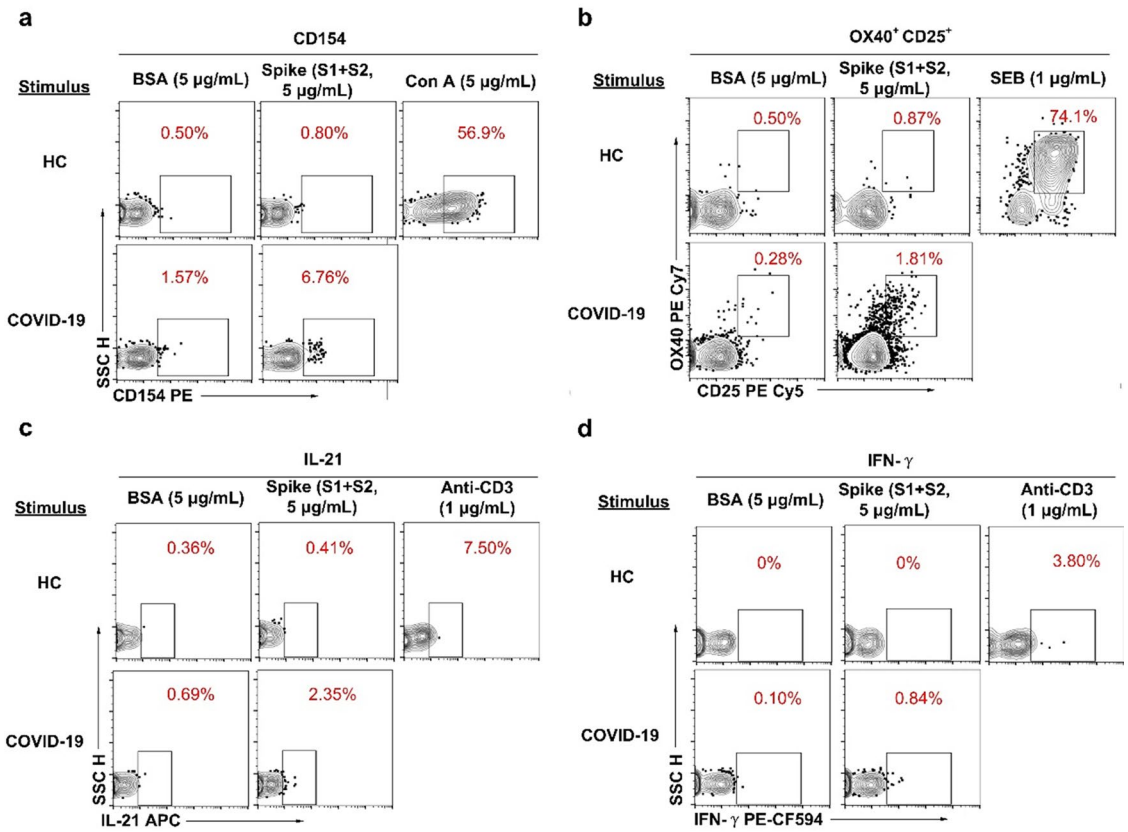

Extended Data Fig. 9 | SARS-CoV-2 spike-specific Tfh cell response after antigen stimulation. Representative flow plots of the antigen specific Tfh cells after stimulation. To determine the expression of CD154 (**a**) and OX40 and CD25 (**b**), PBMCs from COVID-19 individuals and healthy controls were stimulated with SARS-CoV-2 spike subunits S1 and S2, or BSA. Con A and SEB were used as positive controls. After stimulation, surface CD154 and both OX40 and CD25 were measured by flow cytometry gating on PD-1$^+$ CXCR5$^+$ CD4$^+$ T cells. For intracellular cytokine secretion, PBMCs from COVID-19 individuals and healthy controls were stimulated with SARS-CoV-2 spike subunits S1 and S2, or BSA, in the presence of anti-CD28, anti-CD49d. Anti-CD3 was as positive control. After stimulation, intracellular IL-21 (**c**) and IFN-γ (**d**) were measured by flow cytometry gating on PD-1$^+$ CXCR5$^+$ CD4$^+$ T cells. The gating of cell populations was based on the mean fluorescence intensity 'minus one' (FMO).

nature research

Corresponding author(s): Xiaowang Qu

Last updated by author(s): Oct 25, 2020

Reporting Summary

Nature Research wishes to improve the reproducibility of the work that we publish. This form provides structure for consistency and transparency in reporting. For further information on Nature Research policies, see our Editorial Policies and the Editorial Policy Checklist.

Statistics

For all statistical analyses, confirm that the following items are present in the figure legend, table legend, main text, or Methods section.

n/a	Confirmed	
☐	☒	The exact sample size (*n*) for each experimental group/condition, given as a discrete number and unit of measurement
☐	☒	A statement on whether measurements were taken from distinct samples or whether the same sample was measured repeatedly
☐	☒	The statistical test(s) used AND whether they are one- or two-sided *Only common tests should be described solely by name; describe more complex techniques in the Methods section.*
☐	☒	A description of all covariates tested
☐	☒	A description of any assumptions or corrections, such as tests of normality and adjustment for multiple comparisons
☐	☒	A full description of the statistical parameters including central tendency (e.g. means) or other basic estimates (e.g. regression coefficient) AND variation (e.g. standard deviation) or associated estimates of uncertainty (e.g. confidence intervals)
☐	☒	For null hypothesis testing, the test statistic (e.g. *F*, *t*, *r*) with confidence intervals, effect sizes, degrees of freedom and *P* value noted *Give P values as exact values whenever suitable.*
☒	☐	For Bayesian analysis, information on the choice of priors and Markov chain Monte Carlo settings
☒	☐	For hierarchical and complex designs, identification of the appropriate level for tests and full reporting of outcomes
☒	☐	Estimates of effect sizes (e.g. Cohen's *d*, Pearson's *r*), indicating how they were calculated

Our web collection on statistics for biologists contains articles on many of the points above.

Software and code

Policy information about availability of computer code

Data collection	Fluorescence chemiluminescence multifunctional enzyme label instrument （Thermo Varioskan Flash） was used to collect ELISA and luminescence data.MoFlo XDP Flow Cytometer (Beckman Coulter) was used to collect Flow cytometry data.
Data analysis	FlowJo 10.1 was used to analyze Flow cytometry data. SPSS version 26 and GraphPad Prism version 8.0 were used to collected all data and statistical analysis.

For manuscripts utilizing custom algorithms or software that are central to the research but not yet described in published literature, software must be made available to editors and reviewers. We strongly encourage code deposition in a community repository (e.g. GitHub). See the Nature Research guidelines for submitting code & software for further information.

Data

Policy information about availability of data

All manuscripts must include a data availability statement. This statement should provide the following information, where applicable:

- Accession codes, unique identifiers, or web links for publicly available datasets
- A list of figures that have associated raw data
- A description of any restrictions on data availability

All numeral data produced in this study are included as source data. Any other data that support the findings of this study are available from the corresponding author upon request.

Field-specific reporting

Please select the one below that is the best fit for your research. If you are not sure, read the appropriate sections before making your selection.

☒ Life sciences ☐ Behavioural & social sciences ☐ Ecological, evolutionary & environmental sciences

For a reference copy of the document with all sections, see nature.com/documents/nr-reporting-summary-flat.pdf

Life sciences study design

All studies must disclose on these points even when the disclosure is negative.

Sample size	No prior sample size calculation was performed for this human study. N=67 subjects with documented recovered from acute-SARS-CoV-2 infection were included in this study and represented all the patients we were able to recruit in Centre Hospital of Shaoyang, Hunan Province, China.
Data exclusions	No data was excluded from analysis.
Replication	Experiments had at least three, independent, biological replicates and each biological replicate had three technical replicates. All attempts at replication were successful.
Randomization	No specific steps were taken to randomize experimental groups. This is because the classification of patients is clear before recruitment.
Blinding	Blinding was not relevant to our study because the infectious status of the SARS-CoV-2-infected patients has been verified in regard to clinical and experimental data including SARS-CoV-2-RNA as well as anti-SARS-CoV-2 antibodies detection.

Reporting for specific materials, systems and methods

We require information from authors about some types of materials, experimental systems and methods used in many studies. Here, indicate whether each material, system or method listed is relevant to your study. If you are not sure if a list item applies to your research, read the appropriate section before selecting a response.

Materials & experimental systems

n/a	Involved in the study
☐	☒ Antibodies
☐	☒ Eukaryotic cell lines
☒	☐ Palaeontology and archaeology
☒	☐ Animals and other organisms
☐	☒ Human research participants
☐	☒ Clinical data
☒	☐ Dual use research of concern

Methods

n/a	Involved in the study
☒	☐ ChIP-seq
☐	☒ Flow cytometry
☒	☐ MRI-based neuroimaging

Antibodies

Antibodies used

Antibodies used in this study
All antibodies were titrated before staining.
Fluorescent label, Species-targeting, antibody clone, company, cat# number, dilution
BUV737, Mouse anti-human, CD4, SK3, BD Biosciences,564305,2/100
PE, Mouse anti-human, CXCR3, 1C6. BD Biosciences,550633,12/100
FITC, Mouse anti-human, PD-1, EH12.2H7, BioLegend,329904,2/100
PE-eFluor 610, Mouse anti-human. CXCR5, MU5UBEE, Thermo Fisher,61-9185-42,4/100
PE, Mouse anti-human, CD154,24-31, BioLegend,310806,2/100
PE-Cy5, Mouse anti-human, CD25, M-A251, BD Biosciences,555433,6/100
PE-Cy7, Mouse anti-human, OX40, ACT35, BioLegend, 350012,4/100
APC, Mouse anti-human, IL-21,3A3-N2, BioLegend,513008,4/100
PE-CF594, Mouse Anti-Human, IFN-γ, B27, BD Biosciences,562392,4/100
APC, Mouse Anti-Human, CXCR3, G025H7, BioLegend,353708,8/100

Validation

All antibodies were commercially available. Validation statements and citations, available on the manufacturer's websites as following:

BUV737 Mouse anti-Human CD4, Clone SK3
Validation: Each lot of this antibody is quality control tested by staining with flow cytometric analysis.
Citations: Engleman EG, Benike CJ, Glickman E, Evans RL. J Exp Med. 1981; 154(1):193-198.; Evans RL, Wall DW, Platsoucas CD, et al.

Proc Natl Acad Sci U S A. 1981; 78(1):544-548.; Reichert T, DeBruyere M, Deneys V, et al. Clin Immunol Immunopathol. 1991; 60(2):190-208.; Sattentau QJ, Dalgleish AG, Weiss RA, Beverley PC. Science. 1986; 234(4780):1120-1123.; Wood GS, Warner NL, Warnke RA. J Immunol. 1983; 131(1):212-216.
Website: https://www.bdbiosciences.com/cn/reagents/research/antibodies-buffers/immunology-reagents/anti-human-antibodies/cell-surface-antigens/buv737-mouse-anti-human-cd4-sk3-also-known-as-leu3a/p/612748

PE Mouse anti-Human CD183/CXCR3, Clone 1C6
Validation: Each lot of this antibody is quality control tested by staining with flow cytometric analysis.
Citations: Loetscher M, Gerber B, Loetscher P, et al. J Exp Med. 1996; 184(3):963-969.; Piali L, Weber C, LaRosa G, et al. Eur J Immunol. 1998; 28(3):961-972.; Qin S, Rottman JB, Myers P, et al. J Clin Invest. 1998; 101(4):746-754.
Website: https://www.bdbiosciences.com/cn/reagents/research/antibodies-buffers/immunology-reagents/anti-non-human-primate-antibodies/cell-surface-antigens/pe-mouse-anti-human-cd183-1c6cxcr3-also-known-as-1c6-ls177-1c6/p/550633

FITC Mouse anti-human PD-1/CD279, Clone EH12.2H7
Validation: Each lot of this antibody is quality control tested by staining with flow cytometric analysis.
Citations: Jones R, et al. 2009.J Virol.83:8722.; Nakamoto N, et al. 2009. PLoS One. 5:e1000313.; Rueda C, et al. 2015.Hum Immunol.76:65.; Fujigaki J, et al. 2015. PLoS One.10: 0132521.; Ishizaka A, et al. 2016. J Virol. 90: 5665 - 5676.
Website: https://www.biolegend.com/en-us/products/fitc-anti-human-cd279-pd-1-antibody-4411

PE-eFluor 610 Mouse anti-human CD185/CXCR5, Clone MU5UBEE
Validation: Each lot of this antibody is quality control tested by staining with flow cytometric analysis.
Citations: Vaccari M,Fourati S,Gordon SN, et al. Nature medicine, 2018 Jun;24(6):847-856.; Tauriainen J,Scharf L,Frederiksen J, et al. Scientific reports, 2017 Jan 13;7:40354.; Blackburn MJ,Zhong-Min M,Caccuri F, et al. Journal of immunology, 2015 Oct 1;195(7):3227-36.
Website: https://www.thermofisher.com/cn/zh/antibody/product/CD185-CXCR5-Antibody-clone-MU5UBEE-Monoclonal/61-9185-42

PE Mouse anti-human CD154, Clone 24-31
Validation: Each lot of this antibody is quality control tested by intracellular staining with flow cytometric analysis.
Citations: Kuchen S, et al. 2007. J Immunol. 179:5886.; Karnell J, et al. 2011. J Immunol. 187:3603.; Steindor M, et al. 2015. PLoS One. 10:119737.; Yang W, et al. 2019. Nat Med. 25:767.; Shifrut E et al. 2018. Cell. 175(7):1958-1971.; Ahmed R et al. 2019. Cell. 177(6):1583-1599.
Website: https://www.biolegend.com/en-us/products/pe-anti-human-cd154-antibody-1666

PE-Cy 5 Mouse anti-Human CD25, Clone M-A251
Validation: Each lot of this antibody is quality control tested by staining with flow cytometric analysis.
Citations: van Vugt MJ, van den Herik-Oudijk IE, van de Winkle JG. 1996; 88(6):2358-2361.
Website: https://www.bdbiosciences.com/cn/applications/research/t-cell-immunology/regulatory-t-cells/surface-markers/human/pe-cy5-mouse-anti-human-cd25-m-a251/p/555433

PE/Cy7 Mouse anti-Human OX40/CD134, Clone ACT35
Validation: Each lot of this antibody is quality control tested by staining with flow cytometric analysis.
Citations: Colineau L, et al. 2015. PLoS One. 10: e0140978.; Chellappa S, et al. 2016. J Leukoc Biol. 100: 5 - 16.; Dan J, et al. 2016. J Immunol. 197: 983 - 993.; Arce Vargas F et al. 2018. Cancer cell. 33(4):649-663.; Kuo HH et al. 2018. Immunity. 48(6):1183-1194.; Franchini DM et al. 2019. Cell reports. 26(1):94-107.
Website: https://www.biolegend.com/en-us/products/pe-cyanine7-anti-human-cd134-ox40-antibody-7234

APC Mouse anti-Human IL-21, Clone 3A3-N2
Validation: Each lot of this antibody is quality control tested by intracellular staining with flow cytometric analysis.
Citations: Nurieva R. 2007. Nature 448:416.; Parrish-Novak J, et al. 2002. J. Leukocyte Biol. 72:856.; Dumoutier L, et al. 2000. Proc. Natl. Acad. Sci. USA 97:10144.; Asao H, et al. 2001. J. Immunol. 167:1.; Parrish-Novak J, et al. 2000. Nature 408:57.
Website: https://www.biolegend.com/en-us/products/apc-anti-human-il-21-antibody-7779

PE-CF594 Mouse anti-Human IFN-γ, Clone B27
Validation: Each lot of this antibody is quality control tested by intracellular staining with flow cytometric analysis.
Citations: Abrams JS, Roncarolo MG, Yssel H, Andersson U, Gleich GJ, Silver JE. Immunol Rev. 1992; 127:5-24.; Favre C, Wijdenes J, Cabrillat H, Djossou O, Banchereau J, de Vries JE. Mol Immunol. 1989; 26(1):17-25.; Fonteneau JF, Le Drean E, Le Guiner S, Gervois N, Diez E, Jotereau F. J Immunol. 1997; 159(6):2831-2839. Prussin C, Metcalfe DD. J Immunol Methods. 1995; 188(1):117-128.; Rotteveel FT, Kokkelink I, van Lier RA, et al. J Exp Med. 1988; 168(5):1659-1673.
Website: https://www.bdbiosciences.com/cn/applications/research/t-cell-immunology/th-1-cells/intracellular-markers/cytokines-and-chemokines/human/pe-cf594-mouse-anti-human-ifn--b27/p/562392

APC anti-human CXCR3/CD183, Clone G025H7
Validation: Each lot of this antibody is quality control tested by staining with flow cytometric analysis.
Citations: Arlehamn C, et al. 2015. Proc Natl Acad Sci U S A. 112:147.; Yin S, et al. 2015. Sci Rep. 5: 14432.; Pascual–García M, et al. 2019. Nat Commun. 10:2416.; Kubin ME, et al. 2017. Acta Derm Venereol. 97:449.; Zeng W, et al. 2017. Front Immunol. 0.806944444.
Website: https://www.biolegend.com/en-us/products/apc-anti-human-cd183-cxcr3-antibody-7580

Eukaryotic cell lines

Policy information about cell lines

Cell line source(s)	Huh7 were acquired from ATCC.

Authentication	No authentication was performed for Huh7 cells.
Mycoplasma contamination	Huh7 cells tested negative for mycoplasma contamination by us. And anti-mycoplasma drugs were added in culture media avoiding contamination.
Commonly misidentified lines (See ICLAC register)	None of the commonly misidentified cell lines were used in this study.

Human research participants

Policy information about studies involving human research participants

Population characteristics	Of 67 patients, 17 were categorized with severe conditions, and 50 had mild to moderate symptoms (referred to as "non-severe" in this study). The medical histories and the results of physical, hematological, biochemical, radiological, and microbiological analyses were retrospectively evaluated and analyzed. Peripheral blood of the recovered individuals was collected on day 28 after discharge, corresponding to 44 to 52 days after the symptom onset. The baseline characteristics of COVID-19 patients and laboratory findings of COVID-19 patients on admission presented in Extended Data Fig. 1 and 2.
Recruitment	A total of 67 recovered COVID-19 individuals were enrolled in this study, and diagnosis of COVID-19 was made according to WHO interim guidance. All patients presenting as outpatients showed fever or respiratory symptoms; chest computed tomography (CT) scans identified abnormal pulmonary nodules, and SARS-CoV-2 infection was further confirmed using real-time PCR at the local health authority. All patients were hospitalized in the Department of Infectious Disease, The Centre Hospital of Shaoyang, Hunan Province, China, from January 23 to March 2, 2020.
Ethics oversight	This study was performed in accordance with the Good Clinical Practice and the Declaration of Helsinki principles for ethical research. The study protocol was approved by the Institutional Review Board of The Center Hospital of Shaoyang (V1. 0, 20200301), Hunan Province, China. Informed consent was obtained by signing a written consent form from each participant.

Note that full information on the approval of the study protocol must also be provided in the manuscript.

Clinical data

Policy information about clinical studies

All manuscripts should comply with the ICMJE guidelines for publication of clinical research and a completed CONSORT checklist must be included with all submissions.

Clinical trial registration	*Provide the trial registration number from ClinicalTrials.gov or an equivalent agency.*
Study protocol	*Note where the full trial protocol can be accessed OR if not available, explain why.*
Data collection	*Describe the settings and locales of data collection, noting the time periods of recruitment and data collection.*
Outcomes	*Describe how you pre-defined primary and secondary outcome measures and how you assessed these measures.*

Flow Cytometry

Plots

Confirm that:

☒ The axis labels state the marker and fluorochrome used (e.g. CD4-FITC).

☒ The axis scales are clearly visible. Include numbers along axes only for bottom left plot of group (a 'group' is an analysis of identical markers).

☒ All plots are contour plots with outliers or pseudocolor plots.

☒ A numerical value for number of cells or percentage (with statistics) is provided.

Methodology

Sample preparation	To analyze the circulating follicular helper T cells (Tfh) and Tfh subsets, cryopreserved PBMCs were thawed at 37°C water bath and cultured immediately in RPMI 1640 medium supplemented with 10% FBS overnight in 5% CO2 at 37°C. For cell surface staining, 1×106 PBMCs/mL were first labeled with a LIVE/DEAD® Fixable Blue Dead Cell Stain Kit (Thermo Fisher Scientific) to exclude dead cells, and then treated with Fc Block (BioLegend, San Diego, CA, USA) to block non-specific binding. The treated PBMCs were stained with antibodies, which had been pre-titrated and fluorescently labeled, in 96-well V-bottom plates at 4°C for 30 minutes.
Instrument	MoFlo XDP Flow Cytometer (Beckman Coulter, Brea, CA, USA).
Software	FlowJo 10.0 software (Tree Star, San Carlos, CA, USA).

Cell population abundance	Ex vivo analysis, no sorted cells were implicated in this study.
Gating strategy	Cell population gating was set based on the mean fluorescence intensity “minus one” (FMO) and unstained controls.

☒ Tick this box to confirm that a figure exemplifying the gating strategy is provided in the Supplementary Information.